Lawrence Berkeley Laboratory
UNIVERSITY OF CALIFORNIA

Physics Division

Mathematics Department

THREE-DIMENSIONAL VORTEX METHODS

C.A. Greengard
(Ph.D. Thesis)

August 1984

Prepared for the U.S. Department of Energy under Contract DE-AC03-76SF00098

DISCLAIMER

LBL-18217

THREE-DIMENSIONAL VORTEX METHODS[1]

Claude A. Greengard

Department of Mathematics
and
Lawrence Berkeley Laboratory
University of California
Berkeley, California 94720

August 1984

Ph.D. thesis

[1]This work was supported in part by the Applied Mathematical Sciences subprogram of the Office of Energy Research, U.S. Department of Energy under contract DE-AC03-76SF00098.

Three-Dimensional Vortex Methods

Claude A. Greengard

Abstract

Three-dimensional vortex methods for the computation of incompressible fluid flow are presented from a unified point of view. Reformulations of the filament method and of the method of Beale and Majda show them to be very similar algorithms; in both of them, the vorticity is evaluated by a discretization of the spatial derivative of the flow map. The fact that the filament method, the one which is most often used in practice, can be formulated as a version of the Beale and Majda algorithm in a curved coordinate system is used to give a convergence theorem for the filament method.

The method of Anderson is also discussed, in which vorticity is evaluated by the exact differentiation of the approximate velocity field. It is shown that, in the inviscid version of this algorithm, each approximate vector of vorticity remains tangent to a material curve moving with the computed flow, with magnitude proportional to the stretching of this vortex line. This remains true even when time discretization is taken into account.

It is explained that the expanding core vortex method converges to a system of equations different from the Navier-Stokes equations.

Computations with the filament method of the inviscid interaction of two vortex rings are reported, both with single filaments in each ring and with a fully three-dimensional discretization of vorticity. The dependence on parameters is discussed, and convergence of the computed solutions is observed.

Acknowledgements

I wish first of all to thank Alexander Chorin, my thesis advisor, from whose profound insights, wise guidance, and kind encouragement I have greatly benefited.

I also wish to thank Ole Hald and Andy Majda, in whose lectures and, especially, in conversations with whom, I have learned a great deal. Tom Beale has also been a very helpful teacher.

I am grateful to my fellow students Chris Anderson, Robert Krasny, and Mirta Perlman, with whom I have had many informative conversations, and to Phil Colella, Ron Perline, and Enrique Thomann, who made valuable comments to me.

I would like to thank Tony Leonard for sending me a copy of his new review paper prior to publication, and to Paul Schatzle for sending me pictures from his experiments and discussing his work with me, also prior to publication.

CONTENTS

Introduction.

Vortex methods have been successfully used over the past ten years for the study both of inviscid and of slightly viscous flows in two and three dimensions (see, for example, [1],[3],[9],[19],[23],[24],[34],[36], and the review papers [11],[25],[26]). Some convergence results have been obtained recently as well, including convergence proofs for inviscid flows in the absence of boundaries ([2],[5],[6],[16],[21]), and partial results for the viscous flow problem ([4],[15],[27]).

The numerical work has been of two distinctly different kinds. Most of the calculations with vortex methods have involved the simulation of high Reynolds number turbulent flows. These flows depend very sensitively on initial conditions; that is, slight disturbances are enormously amplified in time. Thus, it is impossible to apply numerical approximation procedures to these problems and obtain convergence to the exact solutions. Rather, one aims to represent successfully some of the large-scale features of the flows being studied; optimally, one would like to obtain quantitatively correct information from the calculations. Several experimentally measured quantities have been very well reproduced by finite vortex simulations, and the similarity of the experimental and numerical visualizations of the development of coherent structures in the flows has been striking ([9],[19]).

Accurate calculation of the evolution over shorter intervals of time of less wild flows has also been carried out ([1],[7],[18],[23],[32]), and the numerical work reported here is of this kind. Such calculations have been done both to obtain approximate solutions of the fluid mechanical equations and as a check on the methods and a study of their accuracy. The calculations in [1] and [23] show that the absence of artificial dissipativity of vortex methods allows detailed structures of interfaces to be beautifully resolved. It is not yet clear how much relevance such accurate and short time

calculations with vortex methods have to large-scale simulations, especially in three dimensions. The success of vortex methods in the study of wakes behind circular cylinders, for instance, seems to have more to do with the properties of the infinite-dimensional dynamical system which is the Navier-Stokes equations with the appropriate boundary conditions than with the fact that convergence of particle trajectories can be seen in calculations when small regions of vorticity in free space are covered by hundreds of vortex blobs.

Section 1 contains a discussion about the numerical approximation of the kind of singular integral encountered in the vorticity form of Euler's equations. In Section 2, Euler's equations are introduced and given formulations of which the vortex methods introduced in the following section can be seen as natural discretizations.

Two kinds of three dimensional vortex methods are introduced in Section 3. The first kind, which we call the differential stretching method, requires the exact differentiation of the computational velocity field for the evaluation of the vorticity. This idea was first suggested by Anderson and presented in [2]. A convergence proof has been obtained by Beale ([8]). The second kind of algorithm requires the discretization of the spatial derivative of the computational flow map. Reformulations of the filament method and of the method of Beale and Majda ([5]) given in Section 3 show them both to be of this kind. We call these algorithms discrete stretching methods.

The differential and discrete algorithms are contrasted in Section 4. It is shown there that, although the differential stretching algorithm appears to be noise-producing and hence unattractive, the evaluation of vorticity by the other methods is a discretized version of the evaluation of vorticity by this method. In fact, this method of evaluating the vorticity is the unique one which preserves vortex lines, in the sense discussed in Section 4.

Hald first showed that for two-dimensional Euler flow, appropriate choices of mollifiers for the kernel lead to vortex methods which converge with second-order accuracy in the particle positions ([21]). Beale and Majda proved that arbitrarily high orders of accuracy can be obtained, and that such convergence in particle positions can be obtained not only in two dimensions, but also for their three-dimensional algorithm ([5],[6]).

The filament method can be understood as the method of Beale and Majda in a curved, periodic (in one direction) coordinate system. This fact is used in Section 5 to extend the theory of Beale and Majda, giving a convergence theorem for filament methods.

Modifications of the vortex methods presented in Section 3 are discussed in Section 6. First, it is mentioned that losses of resolution due to vortex stretching can be somewhat remedied by the interpolation of new particles. Second, the simulation of viscosity in vortex methods is discussed. It is explained that the method of random walks ([10]) is applicable to the differential stretching algorithm. The method of core spreading is also discussed, and it is explained that this method converges to a system of equations different from the Navier-Stokes equations.

A fascinating example of vortex motion is the interaction of two initially coplanar (or slightly inclined toward one another), corotating vortex rings. There exist nice experimental visualizations of the ensuing merger of the two rings ([31],[33]); numerical calculations have also been carried out on this model problem ([24],[35]). The numerical work reported in this thesis involves the calculation of the inviscid interaction of the rings. Further calculations of the inviscid and viscous interaction of two rings are underway and will be reported elsewhere.

Solutions obtained by integration of the ordinary differential equation of the vortex method depend on three parameters: the time step Δt, the spatial

discretization parameter h, and the smoothing parameter δ. Solutions obtained in the $h,\Delta t \to 0$ limit are interpreted in Section 7 as solutions of a system of equations called here the E_δ equations, which depend on a smoothing parameter δ and are obtained by smoothing the kernel in the vorticity formulation of Euler's equations. The approach used in our computational work was to obtain accurate solutions of the E_δ equations, in the sense that refinements in h and Δt cause little change in the solution, and to study the behavior of these solutions as δ decreases.

In Section 9, calculations involving resolution of each of the rings by a single filament are discussed. In this case, the solutions depending only on δ are interpreted as weak solutions of the desingularized equations. The limit, as $\delta \to 0$, is necessarily singular, but interesting behavior can be seen for finite values of δ the calculation of which requires only seconds on the VAX 11/780.

Fully three-dimensional vortex ring discretization is discussed in Section 10. In principle, the solutions of the smoothed equations converge to proper solutions of Euler's equations. We have investigated the limiting behavior numerically. Convergence in the center of mass and in the overall ring shapes can be seen. However, it should be noted that slight increases in accuracy require enormous increases in computing time.

1. Discretization of Singular Integrals.

The basis of vortex methods is the discretization of the singular integral which expresses an incompressible vector field as a function of its curl. Before coming to a discussion of fluid mechanics, we consider the problem of discretizing singular integrals in a general setting. Let $K:\mathbb{R}^3\to\mathbb{R}$ be a locally integrable function, unbounded at the origin and smooth elsewhere, let $g:\mathbb{R}^3\to\mathbb{R}$ be bounded and of compact support, and define $f:\mathbb{R}^3\to\mathbb{R}$ by setting

$$f(x)=\int_{\mathbb{R}^3} K(x-\alpha)g(\alpha)d\alpha\,, \tag{1.1}$$

for $x\in\mathbb{R}^3$. Suppose that one would like to obtain approximations to f given finite sets of values of g. Let $\{\alpha_j(h),p_j(h) : j\in J^h\}$ be the set of nodes and weights of some integration formula, so that

$$\lim_{h\to 0}\sum_{j\in J^h} F(\alpha_j(h))p_j(h) = \int_{\mathbb{R}^3} F(\alpha)d\alpha \tag{1.2}$$

for sufficiently smooth functions $F:\mathbb{R}^3\to\mathbb{R}$ of compact support. Fixing x, setting $F(\alpha)=K(x-\alpha)g(\alpha)$, and assuming known the values $g(\alpha_j(h))$ for some given h, the most obvious approximation to $f(x)=\int_{\mathbb{R}^3} F(\alpha)d\alpha$ is

$$f_h(x)=\sum_{j\in J^h} F(\alpha_j)p_j=\sum_{j\in J^h} K(x-\alpha_j)g(\alpha_j)p_j\,, \tag{1.3}$$

where the dependence on h in the notation has been partially suppressed. Unfortunately, the result is a function which, because of the singularity of K, and hence of F, diverges at each node point at which g is nonzero. However small h may be, f_h differs infinitely from f in the L^∞ norm and, unless $K\in L^2_{loc}$, in the L^2 norm as well, even though f is smooth. One can, however, obtain a reasonably accurate approximation to f by replacing K with a bounded function close to K except near the origin. For example, let φ be a function of compact support such that $\int_{\mathbb{R}^3}\varphi=1$, and set $\tilde{K}=K*\varphi$. Then define

the approximation $\tilde{f}_h$ to f by setting

$$\tilde{f}_h(x)=\sum_{j\in J^h}\tilde{K}(x-\alpha_j)g(\alpha_j)p_j\ . \tag{1.4}$$

It is useful to rewrite equations (1.1),(1.3) and (1.4) as convolutions of K with the appropriate distributions, in order to understand the approximations better. Let g_h be the singular distribution $g_h(x)=\sum_{j\in J^h} g(\alpha_j)\delta_0(x-\alpha_j)p_j$, where δ_0 is the Dirac delta distribution concentrated at the origin, and define $\tilde{g}_h(x)=\sum_{j\in J^h} g(\alpha_j)\varphi(x-\alpha_j)p_j$. The associativity of the convolution operator implies

$$f=K*g$$
$$f_h=K*g_h$$
$$\tilde{f}_h=K*\tilde{g}_h\ .$$

The closer the cutoff function φ is to the Dirac distribution, the more singular $\tilde{f}_h$ becomes. However, for appropriate one-parameter families of cutoff functions φ_δ approaching the Dirac distribution as $\delta\to 0$, the approximations

$$\sum_{j\in J^h}(K*\varphi_\delta)(x-\alpha_j(h))g(\alpha_j(h))p_j(h) \tag{1.5}$$

approach $f(x)$ uniformly in x as $\delta,h\to 0$ provided that K and g satisfy certain conditions, and that h tends to zero more quickly than δ. Theorem 1.1 provides an example.

The approximation by (1.5) is not sufficiently general to cover the case of interest to us in fluid mechanics. For application to the vortex method, one would like to approximate f accurately given the values of g, not on the set of nodes α_i of a nice integration formula, but rather on the set of images $\Psi(\alpha_j)$ of these nodes under a smooth, measure-preserving transformation $\Psi:\mathbb{R}^3\to\mathbb{R}^3$. Changing variables in the integral in (1.1), we get

$$f(x)=\int_{\mathbb{R}^3} K(x-\Psi(\alpha))g(\Psi(\alpha))d\alpha\,. \tag{1.6}$$

Set $K_\delta=K*\varphi_\delta$. The approximation to f analogous to (1.5) is the function $f_{\delta,h}$ defined by

$$f_{\delta,h}(x)=\sum_{j\in J^h} K_\delta(x-\Psi(\alpha_j))\,g(\Psi(\alpha_j))\,p_j\,. \tag{1.7}$$

In fact, one can obtain a converging approximation scheme in this way. This is the content of Theorem 1.1, which follows ideas in ([2],[5],[17]). In order to prove that $f_{\delta,h}$ is an accurate approximation to f, it is convenient to obtain the approximate identity $\{\varphi_\delta\}$ from a fixed function φ of integral one through the relation

$$\varphi_\delta(x)=\frac{1}{\delta^3}\varphi(x/\delta)\,. \tag{1.8}$$

A class of functions φ for which the proof of Theorem 1.1 holds is defined next.

Definition. The class $M^{l,p}$ is the collection of functions $\varphi\in C^l(\mathbb{R}^3)$ such that $\int_{\mathbb{R}^3}\varphi=1$, which in addition satisfy the following conditions:

(i) $\int_{\mathbb{R}^3} x^\alpha\varphi(x)dx=0$, for all multi-indices α such that $1\le|\alpha|\le p-1$

$\int_{\mathbb{R}^3}|x|^p|\varphi(x)|dx<\infty$

(ii) $|x|^{3+|\beta|}|D^\beta\varphi(x)|\le C$ for some C, and all β s.t. $|\beta|\le l$

(iii) $|x|^{p+5}|\varphi(x)|\le C$ for some constant C

In the following, when A is a region in $\mathbb{R}^3$ and F is a real-valued function on A, we use the notation

$$\|F\|_{W^{l,p}(A)}=\max_{|\beta|\le l}\|D^\beta F\|_{L^p(A)}\,.$$

In Theorem 1.1, we assume that K is one of the functions $x_i/|x|^3$, $i=1,2$, or

3, although the convergence of the approximation scheme (1.7) can be shown to hold for a wider class of kernels.

We restrict our attention now to the trapezoidal rule, obtained by setting $J^h=\mathbb{Z}^3$, for all h, and $\alpha_j(h)=h\cdot j=h\cdot(j_1,j_2,j_3)$, $p_j(h)=h^3$, for all j. Of course, the sum in (1.2) is finite since for all but finitely many j, $F(h\cdot j)=0$. It is proved in [2] that for each integer $l\geq 4$, and all functions $F\in C^l(\mathbb{R}^3)$ of compact support,

$$\left| \int_D F(y)dy - \sum_{j\in\mathbb{Z}^3} F(h\cdot j)h^3 \right| \leq \frac{52}{(2\pi)^l} \| F \|_{W^{l,1}(D)} h^l \,. \tag{1.9}$$

Theorem 1.1 Let $D \subset \mathbb{R}^3$ be a bounded region, and assume $g\in C^l(\mathbb{R}^3)$, with $supp(g) \subset D$. Assume $\Psi\in C^l(\mathbb{R}^3)$, and let f and $f_{\delta,h}$ be defined as in (1.6)-(1.7). Assume further that $\varphi\in M^{L,p}$. Then for some constant C which depends only on l, $\| \Psi \|_{W^{l,\infty}(\Psi^{-1}(D))}$, $\| g \|_{W^{l,\infty}(D)}$, and the diameter of D,

$$\| f - f_{\delta,h} \|_{L^\infty(\mathbb{R}^3)} \leq C(\delta^p + h^l \delta^{l-1}) \,.$$

Proof: Define

$$f_\delta(x)=\int K_\delta(x-\Psi(\alpha))g(\Psi(\alpha))d\alpha \,,$$

for $x\in\mathbb{R}^3$. It is shown in [6] that for some constant C,

$$\| f - f_\delta \|_{L^\infty(\mathbb{R}^3)} \leq C\delta^p \,.$$

All that is left is to estimate $f_\delta - f_{\delta,h}$, which is the error in discretizing the integral of the smooth function

$$F(\alpha)=K_\delta(x-\Psi(\alpha))g(\Psi(\alpha))$$

by the given integration formula. By repeated application of the chain rule and the product rule, it follows that derivatives of F up to order l are sums of derivatives of K_δ up to order l multiplied by derivatives up to order l of Ψ and g. Hence, for some constant C'_l which depends only on l,

$$\| F \|_{W^{l,1}(D)} \le C'_l \| K_\delta \|_{W^{l,1}(x-D)} \| g \|_{W^{l,\infty}(D)} \max_{1 \le k \le l} \| \Psi \|^k_{W^{l,\infty}(\Psi^{-1}(D))} .$$

Since the integral of K_δ over any compact set is bounded by a constant multiple of δ^{1-l} (see [2]), with the constant depending only on φ and on the diameter of the set,

$$\| f_{\delta,h} - f_\delta \|_{L^\infty(\mathbb{R}^3)} \le \frac{52}{(2\pi)^l} \| F \|_{W^{l,1}(D)} h^l \le C_2 \delta^{1-l} h^l ,$$

for some constant C_2. Thus,

$$\| f - f_{\delta,h} \|_{L^\infty(\mathbb{R}^3)} \le \| f - f_\delta \|_{L^\infty(\mathbb{R}^3)} + \| f_\delta - f_{\delta,h} \|_{L^\infty(\mathbb{R}^3)} \le C(\delta^p + \delta^{1-l} h^l).$$

2. Euler's Equations.

The three-dimensional Euler equations in vorticity formulation are

$$\begin{aligned} &\omega(x,0)=\eta(x)\,, \\ &\partial_t\omega+(u\cdot\nabla)\omega=(\omega\cdot\nabla)u\,, \\ &u=K*\omega\,, \end{aligned} \tag{2.1}$$

where K is the matrix

$$K(x) = \frac{1}{4\pi}\begin{pmatrix} 0 & \frac{x_3}{|x|^3} & \frac{-x_2}{|x|^3} \\ \frac{-x_3}{|x|^3} & 0 & \frac{x_1}{|x|^3} \\ \frac{x_2}{|x|^3} & \frac{-x_1}{|x|^3} & 0 \end{pmatrix}.$$

Assume that η is sufficiently smooth and that $[0,T]$ is a sufficiently short interval of time so that a smooth solution to (2.1) exists ([22]). The flow map $\Phi:\mathbb{R}^3\times[0,T]\to\mathbb{R}^3$ is defined by

$$\begin{aligned} &\Phi(\alpha,0)=\alpha\,, \\ &\frac{\partial}{\partial t}\Phi(\alpha,t)=u(\Phi(\alpha,t),t)\,. \end{aligned} \tag{2.2}$$

We shall use the notation

$$\begin{aligned} \Phi_\alpha(t)&=\Phi(\alpha,t)\,, \\ \omega_\alpha(t)&=\omega(\Phi_\alpha(t),t)\,, \end{aligned}$$

for $\alpha\in\mathbb{R}^3$ and $t\in[0,T]$. The two different numerical methods we discuss below will be motivated by different formulations of the evolution equation for the $\omega_\alpha(t)$. It follows by the chain rule from the second equation in (2.1) that for all α,

$$\frac{d}{dt}\omega_\alpha(t) = (\omega_\alpha(t)\cdot\nabla)u\,(\Phi_\alpha(t),t)\,. \tag{2.3}$$

An equivalent equation governing vorticity evolution along particle trajectories is

$$\omega_a(t)=\left[D_a\Phi(\alpha,t)\right]\cdot\omega(\alpha,0)=\left[D_a\Phi(\alpha,t)\right]\cdot\eta(\alpha)\,, \tag{2.4}$$

where $D_a\Phi$ is the 3×3 matrix of partial derivatives of Φ with respect to the spatial variables α, and the dot denotes the product of matrix and vector (see [14]).

It follows from the third equation in (2.1) that the flow map is measure-preserving, and a change of variables yields

$$u(x,t)=\int K(x-y)\omega(y,t)dy=\int K(x-\Phi_a(t))\omega_a(t)d\alpha\,. \tag{2.5}$$

Define $U[\Psi,\Omega]:\mathbb{R}^3\to\mathbb{R}^3$, for $\Psi,\Omega:\mathbb{R}^3\to\mathbb{R}^3$, to be the vector field

$$U[\Psi,\Omega](x)=\int K(x-\Psi(\alpha))\Omega(\alpha)d\alpha\,. \tag{2.6}$$

When X is defined on $(x,t)\in\mathbb{R}^3\times[0,T]$, we shall denote by $X(t)$ the function $X(t)(x)=X(x,t)$. Then (2.5) can be written in the form

$$u(x,t)=U[\Phi(t),\omega(t)](x)\,.$$

Using equations (2.2)-(2.6), we give two Lagrangian formulations of the equations of motion, on which the two vortex methods described in the next section are based. System A is the set of equations

$$\Phi(\alpha,0)=\alpha\,,$$

$$\frac{d}{dt}\Phi_a(t)=U[\Phi(t),\omega(t)](\Phi_a(t))\,,$$

$$\omega_a(0)=\eta(\alpha)\,,$$

$$\frac{d}{dt}\omega_a(t)=(\omega_a(t)\cdot\nabla)U[\Phi(t),\omega(t)](\Phi_a(t))\,,$$

and system B is the set of equations

$$\Phi(\alpha,0)=\alpha\ ,$$

$$\frac{d}{dt}\Phi_\alpha(t)=U[\Phi(t),\omega(t)](\Phi_\alpha(t))\ ,$$

$$\omega_\alpha(t)=\left[D_\alpha\Phi(\alpha,t)\right]\cdot\eta(\alpha)\ .$$

3. Three-Dimensional Vortex Methods.

We discretize the systems of equations A and B, in order to compute solutions to Euler's equations, by tracking the positions of a finite number of particles (called vortices), and keeping track of vortex stretching along the trajectories of these particles. Denote by J^h a set by which the vortices are indexed; h typically represents the distance between neighboring initial vortex positions. For each $i \in J^h$, we denote by α_i the initial position of the i^{th} vortex, and by $\Phi_i^{\delta,h}(t)$ and $\omega_i^{\delta,h}(t)$ approximations to $\Phi_{\alpha_i}(t)$ and $\omega_{\alpha_i}(t)$, respectively. Let each initial position α_i be assigned a corresponding weight p_i. Set $K_\delta = K * \varphi_\delta$, with φ_δ defined as in (1.8). In the light of the discussion in Section 1, it seems reasonable to approximate $U[\Phi(t),\omega(t)]$ by $U_{\delta,h}[\Phi^{\delta,h}(t),\omega^{\delta,h}(t)]$, where $U_{\delta,h}[\Psi,\Omega]$ is the vector field defined for $\Psi,\Omega:\{\alpha_i : i \in J^h\} \to \mathbb{R}^3$ by setting

$$U_{\delta,h}[\Psi,\Omega](x) = \sum_{i \in J^h} K_\delta(x - \Psi(\alpha_i))\Omega(\alpha_i)p_i \,. \tag{3.1}$$

There are numerous functions φ (even in the class $M^{l,p}$) for which the modified kernels K_δ can be exhibited explicitly (see [7]); this fact permits straightforward implementation of the numerical algorithms discussed below. We mention that if φ has support contained within the unit ball, then $K_\delta(x) = K(x)$ for $|x| \geq \delta$; if φ has only radial dependence, then $K_\delta(0) = 0$. We describe now two vortex methods, which differ only in their evaluations of the vortex stretching, and which we call the differential and discrete algorithms.

Differential stretching method: The system of ordinary differential equations

$$\Phi_i^{\delta,h}(0) = \alpha_i \,, \tag{3.2}$$

$$\frac{d}{dt}\Phi_i^{\delta,h}(t) = U_{\delta,h}[\Phi^{\delta,h}(t),\omega^{\delta,h}(t)]\,(\Phi_i^{\delta,h}(t))\,, \tag{3.3}$$

$$\omega_i^{\delta,h}(0) = \eta(\alpha_i)\,, \tag{3.4}$$

$$\frac{d}{dt}\omega_i^{\delta,h}(t) = (\omega_i^{\delta,h}(t)\cdot\nabla)U_{\delta,h}[\Phi^{\delta,h}(t),\omega^{\delta,h}(t)]\,(\Phi_i^{\delta,h}(t))\,, \tag{3.5}$$

is a discretization of system A, and we call it the differential algorithm. The approximate vector field $U_{\delta,h}$ is exactly differentiated here, the implementation of which procedure requires only differentiation of the explicit representation of K_δ. This vortex method is presented in [2].

Discrete stretching method: Most of the three-dimensional algorithms which have been used in practice, although introduced by other authors in a different way, can be understood as discretizations of system B. We call these methods filament algorithms and discuss them below. One can approximate B by coupling equations (3.2)-(3.3) with a formula which determines vortex stretching by replacing the spatial derivative of the flow map in (2.4) with a finite difference approximation to this derivative. We discuss two different implementations of this idea.

Filament Algorithms: In these algorithms, vortex structures at time $t=0$ are approximated by one or more vortex filaments. Each filament is discretized by choosing points α_i along the filaments with roughly equal spacings between them. This initialization procedure allows the derivative of the flow map in the filamental direction to be approximated by taking finite differences along the filament. For instance, approximating $\eta(\alpha_i)$ by $c_i\frac{(\alpha_{i+1}-\alpha_{i-1})}{2h}$, one can set

$$\omega_i^{\delta,h}(t)=c_i\frac{(\Phi_{i+1}^{\delta,h}(t)-\Phi_{i-1}^{\delta,h}(t))}{2h}. \tag{3.6}$$

Mesh Algorithms: Alternatively, one can choose the vortices to lie, initially, on the nodes of a rectangular grid. In this case, one must approximate partial derivatives of the flow map in all three orthogonal directions, since the vorticity will in general not be aligned exactly along the coordinate axes. Recalling that $\Phi_i^{\delta,h}(t)$ is an approximation to $\Phi(\alpha_i,t)$, one sets

$$\omega_i^{\delta,h}(t) = \left[D_\alpha^h\Phi_i^{\delta,h}(t)\right]\cdot\eta(\alpha_i)\,. \tag{3.7}$$

where D_α^h is a finite difference approximation to the spatial derivative. This turns out to be the algorithm suggested by Beale and Majda, though they define the $\omega_i^{\delta,h}(t)$ by coupling to equations (3.2) and (3.3) the differential equations

$$\omega_i^{\delta,h}(0)=\eta(\alpha_i) \tag{3.8}$$

$$\frac{d}{dt}\omega_i^{\delta,h}(t)=\left[D_\alpha^h\left(U_{\delta,h}[\Phi^{\delta,h}(t),\omega^{\delta,h}(t)]\circ\Phi_i^{\delta,h}(t)\right)\right]\cdot\eta(\alpha_i)\,. \tag{3.9}$$

It can easily be checked that (3.9) is the derivative in time of (3.7).

The mesh and the filament method each has certain advantages over the other. It is conceptually nicer to have vorticity aligned along vortex lines. Moreover, more particle trajectories need to be computed with a mesh initialization than with a vortex line initialization, for with a mesh initialization all nearest neighbors of all nodes at which the initial vorticity is nonzero must be tracked in time in order for the vortex stretching to be evaluated. If one starts with a vorticity distribution which is fairly thin, a substantial increase in computational work results. On the other hand, given an initial vorticity distribution as an arbitrary function of space, the mesh algorithm is by far the easier to implement.

4. Discrete Stretching Versus Differential Stretching.

It is well known that the differentiation of interpolated functions is a dangerous numerical procedure. Thus, the differential algorithm, which requires the differentiation of the interpolated vector field $U_{\delta,h}$, appears at first glance to be noisier than the discrete one. In fact, as is shown below, the differential and discrete algorithms are surprisingly close to one another.

Given the vortex trajectories $(\Phi_i^{\delta,h}(t),\omega_i^{\delta,h}(t))$ which form the solution to the autonomous ordinary differential equation of either algorithm, we define an approximate flow map $\Phi^{\delta,h}:\mathbb{R}^3\times[0,T]\to\mathbb{R}^3$ as the solution of the nonautonomous ordinary differential equation

$$\Phi^{\delta,h}(\alpha,0)=\alpha\ ,$$

$$\frac{\partial}{\partial t}\Phi^{\delta,h}(\alpha,t)=U_{\delta,h}[\Phi^{\delta,h}(t),\omega^{\delta,h}(t)]\,(\Phi^{\delta,h}(\alpha,t))\ . \tag{4.1}$$

This notation is consistent for, as a comparison of equation (3.3) with equation (4.1) reveals,

$$\Phi^{\delta,h}(\alpha_i,t)=\Phi_i^{\delta,h}(t)\ .$$

Thus, $\Phi^{\delta,h}(t)$ is a measure-preserving flow which agrees on the Lagrangian variables α_i with the approximate particle trajectories of the algorithm.

The following result shows that the relationship between the flow map and vorticity that holds in Euler flow holds also in the differential algorithm. In particular, vortex lines are preserved by the flow of the differential algorithm, in the sense that the vorticity calculated in the algorithm is always tangent to the same material curve in the fluid, and the magnitude of the vorticity is always in proportion to the stretching of this "vortex line".

Proposition 4.1 Let $\Phi^{\delta,h}$ be a flow map of the differential algorithm. Then for each i,

$$\omega_i^{\delta,h}(t)=\left[D_a\Phi^{\delta,h}(\alpha_i,t)\right]\cdot\eta(\alpha_i)\,. \tag{4.2}$$

Proof: Define

$$\xi_i(t)=\left[D_a\Phi^{\delta,h}(\alpha_i,t)\right]\cdot\eta(\alpha_i)\,.$$

Then

$$\begin{aligned}\frac{d}{dt}\xi_i(t)&=\left[D_a\frac{\partial\Phi^{\delta,h}}{\partial t}(\alpha_i,t)\right]\cdot\eta(\alpha_i)\\&=\left[D_aU_{\delta,h}[\Phi^{\delta,h}(t),\omega^{\delta,h}(t)](\Phi^{\delta,h}(\alpha_i,t))\right]\cdot\eta(\alpha_i)\\&=\left(\left(\left[D_a\Phi^{\delta,h}(\alpha_i,t)\right]\cdot\eta(\alpha_i)\right)\cdot\nabla\right)\left(U_{\delta,h}[\Phi^{\delta,h}(t),\omega^{\delta,h}(t)]\right)\left(\Phi_i^{\delta,h}(t)\right)\\&=(\xi_i(t)\cdot\nabla)(U_{\delta,h}[\Phi^{\delta,h}(t),\omega^{\delta,h}(t)])\,(\Phi_i^{\delta,h}(t))\,.\end{aligned}$$

Moreover, since

$$\omega_i^{\delta,h}(0)=\eta(\alpha_i)=\xi_i(0)\,,$$

and since

$$\frac{d}{dt}\omega_i^{\delta,h}(t)=(\omega_i^{\delta,h}(t)\cdot\nabla)\,(U_{\delta,h}[\Phi^{\delta,h}(t),\omega^{\delta,h}(t)])\,(\Phi_i^{\delta,h}(t))\,,$$

ξ_i and $\omega_i^{\delta,h}$ satisfy the same ordinary differential equation and hence are identical.

We summarize by displaying the Lagrangian vortex stretching formulas for the Euler equations and for the discrete and differential vortex methods:

Euler: $$\omega_{\alpha_i}(t)=\left[D_\alpha\Phi(\alpha_i,t)\right]\cdot\eta(\alpha_i)$$

Differential: $$\omega_i^{\delta,h}(t)=\left[D_\alpha\Phi^{\delta,h}(\alpha_i,t)\right]\cdot\eta(\alpha_i)$$

Discrete: $$\omega_i^{\delta,h}(t)=\left[D_\alpha^h\Phi^{\delta,h}(\alpha_i,t)\right]\cdot\eta(\alpha_i)$$

Thus, we see that although the systems of ordinary differential equations that constitute the differential and discrete methods appear very different, the transformation of vorticity by the approximate flow map in the discrete algorithm differs from that in the differential algorithm only in that a discretized version of the spatial derivative of $\Phi^{\delta,h}$, rather than the real derivative, is applied to the initial vorticity. This is why we have chosen to call the methods discrete and differential, rather than Lagrangian and Eulerian, respectively.

Proposition 4.1 can be strengthened. For, the analogous result holds even when the ordinary differential equations are replaced by difference approximations. Proposition 4.2 is the statement of this fact for Euler's method of integration in time; similar statements hold for the other Runge-Kutta methods.

For each vortex index i, denote by $\Phi_i^{\delta,h,n}$ and $\omega_i^{\delta,h,n}$ the particle positions and vorticity values, respectively, of the i^{th}-particle at time $n\Delta t$ obtained by solving the system of equations (3.2)-(3.5) by Euler's method with time steps of size Δt. The natural flow map which agrees with the vortex trajectories is defined at discrete times by setting

$$\Phi^{\delta,h,0}(\alpha)=\alpha \tag{4.3}$$

and, recursively,

$$\Phi^{\delta,h,n+1}(\alpha)=\Phi^{\delta,h,n}(\alpha)+\Delta t\, U_{\delta,h}[\Phi^{\delta,h,n},\omega^{\delta,h,n}](\Phi^{\delta,h,n}(\alpha)). \tag{4.4}$$

Proposition 4.2 For each integer n, let $\Phi^{\delta,h,n}:\mathbb{R}^3\to\mathbb{R}^3$ be the transformation defined by (4.3)-(4.4). Then

$$\omega_i^{\delta,h,n}=\left(D_\alpha\Phi^{\delta,h,n}(\alpha_i)\right)\cdot\eta(\alpha_i) \tag{4.5}$$

Proof: The proof is by induction. The case $n=0$ of (4.5) is true by definition. Let n be an integer for which (4.5) holds. Then

$$\begin{aligned}
\left(D_\alpha\Phi^{\delta,h,n+1}(\alpha_i)\right)\cdot\eta(\alpha_i)&=\left(D_\alpha\Phi^{\delta,h,n}(\alpha_i)\right)\cdot\eta(\alpha_i)+\left(D_\alpha(\Phi^{\delta,h,n+1}(\alpha_i)-\Phi^{\delta,h,n}(\alpha_i))\right)\cdot\eta(\alpha_i)\\
&=\omega_i^{\delta,h,n}+\left(D_\alpha(\Delta t\, U_{\delta,h}[\Phi^{\delta,h,n},\omega^{\delta,h,n}](\Phi_i^{\delta,h,n}))\right)\cdot\eta(\alpha_i)\\
&=\omega_i^{\delta,h,n}+\Delta t\,((\left(D_\alpha\Phi^{\delta,h,n}(\alpha_i)\right)\cdot\eta(\alpha_i))\cdot\nabla)U_{\delta,h}[\Phi^{\delta,h,n},\omega^{\delta,h,n}](\Phi_i^{\delta,h,n})\\
&=\omega_i^{\delta,h,n}+\Delta t\,(\omega_i^{\delta,h,n}\cdot\nabla)U_{\delta,h}[\Phi^{\delta,h,n},\omega^{\delta,h,n}](\Phi_i^{\delta,h,n})\\
&=\omega_i^{\delta,h,n+1}
\end{aligned}$$

5. Convergence of Filament Method.

In this section, we extend the convergence theorem of Beale and Majda, which applies to the mesh algorithm, and show that filament methods converge with high orders of accuracy.

We assume that smooth solutions to Euler's equations exist on some interval of time [0,T]. We denote by A the support of the initial vorticity η, which we assume is compact.

In order to prove that filament methods converge, one needs to show that one can obtain both an accurate integration formula and an accurate discrete approximation to the spatial derivative when computational elements are placed initially along curves rather than on the nodes of rectangular grids. This can be accomplished by transforming a rectangular coordinate system to a curved coordinate system, with straight lines parallel to one of the axes of the rectangular coordinate system mapped to vortex filaments.

We introduce now some more notation. Let $\{\alpha_j(h),p_j(h),j\in J^h\}$ be an integration formula for a region $D'\subseteq \mathbb{R}^3$, as in (1.2). We define the discrete L^2 norm for regions $D\subseteq D'$ and functions g defined on the set of $\alpha_i\in D$, by setting

$$\| g \|^2_{L^2_h(D)} = \sum_{\alpha_i\in D} | g(\alpha_i(h)) |^2 p_i(h) .$$

The dependence of α_i and p_i on h shall be suppressed occasionally in the notation.

Before discussing convergence theory for filament methods, we review the theorem of Beale and Majda ([5],[6]) and sketch their proof (with a slight improvement).

Thus, we restrict our attention for the moment to the mesh algorithm. Set $J^h=\mathbb{Z}^3$, and $\alpha_i(h) = h\cdot i = h\cdot(i_1,i_2,i_3)$, $p_i(h)=h^3$, for all $i\in J^h$. Let $D\supset A$

be a bounded, open set, and let D_a^h be a finite difference operator of r^{th} order accuracy. The system of ordinary differential equations which constitutes the mesh algorithm is

$$\Phi_i^{\delta,h}(0) = \alpha_i \,, \tag{5.1}$$

$$\frac{d}{dt}\Phi_i^{\delta,h}(t) = U_{\delta,h}[\Phi^{\delta,h}(t),\omega^{\delta,h}(t)]\,(\Phi_i^{\delta,h}(t)) \,, \tag{5.2}$$

for $i \in J^h$ such that $\alpha_i \in D$, where $U_{\delta,h}$ is defined so that

$$U_{\delta,h}[\Psi,\Omega]\,(x) = \sum_{\alpha_i \in A} K_\delta(x-\Psi(\alpha_i))\Omega(\alpha_i)\,p_i \,, \tag{5.3}$$

for $\Psi,\Omega:\{\alpha_i \in D\} \to \mathbb{R}^3$, and where

$$\omega_i^{\delta,h}(t) = \left[D_a^h \Phi^{\delta,h}(t)\,(\alpha_i)\right]\cdot\eta(\alpha_i) \,, \tag{5.4}$$

for $\alpha_i \in A$. a finite difference operator of r^{th} order accuracy. The reason for the inclusion of initial particle positions α_i outside of A, which consequently carry no vorticity, is that the evaluation of the vorticity by (5.4) requires knowledge of the positions of particles which, at time $t=0$, are neighbors of node points $\alpha_i \in A$.

Consistency:

Let U be defined as in (2.6) and suppose that the cutoff function $\varphi \in M^{l,p}$, with $l \geq 4$. It follows from Theorem 1.1 that

$$\| U[\Phi(t),\omega(t)] - U_{\delta,h}[\Phi(t),\omega(t)] \|_{L^\infty(\mathbb{R}^3)} \leq C\,(\delta^p + h^l \delta^{1-l}) \,. \tag{5.5}$$

Thus, the errors in velocity due to the replacement of the integral over a smooth vorticity field by a finite summation can be made arbitrarily small by letting h and δ tend to zero, keeping δ sufficiently larger than h.

In order to prove that the vortex method converges, it is convenient to convert the estimate (5.5) into an L_h^2 norm estimate. Since D is a bounded region, L^p norms on D are bounded by constants times L^q norms for $p < q$.

The corresponding fact also holds for the discrete norms, and in particular, for any function g on D,

$$\| g \|_{L^2_h(D)} \leq \left(\frac{\pi}{3}(diam(D)+\sqrt{3}h)^3\right)^{1/2} \| g \|_{L^\infty(D)} . \tag{5.6}$$

where $diam(D)$ is the diameter of D. Define the Lagrangian vector fields

$$V[\Psi,\Omega](\alpha)=U[\Psi,\Omega](\Psi(\alpha)) \quad \text{and} \quad V_{\delta,h}[\Psi,\Omega](\alpha)=U_{\delta,h}[\Psi,\Omega](\Psi(\alpha)) .$$

It follows from (5.5) and (5.6) that for some constant C independent of h and δ, and for all sufficiently small h,

$$\| V[\Phi(t),\omega(t)]-V_{\delta,h}[\Phi(t),\omega(t)] \|_{L^2_h(A)} \leq C(\delta^p+h^l\delta^{l-1}) . \tag{5.7}$$

Stability:

The convergence proof also requires that the approximation of the velocity by $U_{\delta,h}$ be stable. The original proof of the stability of vortex methods is due to Hald ([21]), who showed that in two dimensions, perturbations in induced velocity are bounded by perturbations in particle positions. Beale and Majda proved the stability of three-dimensional vortex methods, showing that errors in velocity are bounded by errors in particle positions and in vorticity. In order to state their stability result, we need to introduce a discretized version of the Sobolev $W^{-1,2}$ norm. Let g be defined on the set of α_j contained in D. Then we set

$$\| g \|_{W^{-1,2}_h(D)} = sup \frac{| \sum_{\alpha_i \in D} g(\alpha_i)\cdot\gamma(\alpha_i)h^3 |}{\| \gamma \|^2_{L^2_h(\mathbb{R}^3)}+\sum_{k=1}^{3} \| D_k^+\gamma \|^2_{L^2_h(\mathbb{R}^3)}},$$

where the supremum is over all functions γ defined on J^h, and D_k^+ denotes the forward difference operator in the k^{th} direction. Beale and Majda show that there is a constant C such that for all $t\in[0,T]$, all $\Psi:J^h\to\mathbb{R}^3$ such that $\| \Psi-\Phi(t) \|_{L^2_h(D)} \leq h^3$, and all $\Omega:J^h\to\mathbb{R}^3$,

(5.8)

$$\| V_{\delta,h}[\Phi(t),\omega(t)]-V_{\delta,h}[\Psi,\Omega] \|_{L^2_h(D)} \le C(\| \Phi(t)-\Psi \|_{L^2_h(D)} + \| \omega(t)-\Omega \|_{W_h^{-1,2}(A)}) .$$

Since D_α^h is a of r^{th}-order accuracy,

$$\| \omega(t)-\left(D_\alpha^h\Phi(t)\right)\cdot\eta \|_{W_h^{-1,2}(A)} = \| \left((D_\alpha-D_\alpha^h)\Phi(t)\right)\cdot\eta \|_{W_h^{-1,2}(A)} \le Ch^r . \qquad (5.9)$$

Consistent difference operator approximations to the derivative yield bounded operators from L_h^2 to $W_h^{-1,2}$ (see [5]). Hence,

$$\| \left(D_\alpha^h\Phi(t)\right)\cdot\eta-\left(D_\alpha^h\Phi^{\delta,h}(t)\right)\cdot\eta \|_{W_h^{-1,2}(A)} \le C' \| D_\alpha^h(\Phi(t)-\Phi^{\delta,h}(t)) \|_{W_h^{-1,2}(A)} \qquad (5.10)$$

$$\le C \| \Phi(t)-\Phi^{\delta,h}(t) \|_{L^2_h(D)} .$$

Thus,

(5.11)

$$\| V_{\delta,h}[\Phi(t),\omega(t)]-V_{\delta,h}[\Phi^{\delta,h}(t),\omega^{\delta,h}(t)] \|_{L^2_h(D)} \le C(\| \Phi(t)-\Phi^{\delta,h}(t) \|_{L^2_h(D)}+h^r) .$$

The convergence of the particle trajectories of the vortex method to the exact trajectories can be proved using (5.7) and (5.11), as is done in [2] (with only slight changes from [5]). Convergence estimates for the vortex method integrated in time by 1^{st} or 2^{nd} order Runge-Kutta methods are obtained in [2].

In order to prove convergence of the filament method, we consider Sobolev spaces on subsets of $\mathbb{R}^3$ which are periodic in one direction. Set $S=\mathbb{R}^2\times[0,2\pi]$. For each $h=2\pi/n$, where n is an integer, we set $\tilde{\alpha}_i(h)=h\cdot(i_1,i_2,i_3)$ and $\tilde{p}_i(h)=h^3$. The restriction on h and the identification of the edges $\mathbb{R}^2\times\{0\}$ and $\mathbb{R}^2\times\{2\pi\}$ makes it clear how to define the W_h^{-1} space for the set S. Moreover, if D_α^h is any difference operator on $\mathbb{R}^3$, one can define it near the endpoints of the cylinder S by periodicity and in this way obtain an accurate difference operator on S.

Let $B \subset \mathbb{R}^2$ be compact and let $X:E \to A$ be a diffeomorphism from the compact set $E=B\times[0,2\pi] \subset D$ onto the support of the vorticity field at time $t=0$. We denote by $|D_{\tilde{\alpha}}X(\tilde{\alpha})|$ the Jacobian of X at the point $\tilde{\alpha}=(b,\varphi)$. Set $J^h=\{i\in\mathbb{Z}^3:\tilde{\alpha}_i(h)\in E\}$. We obtain an integration formula on A, inherited from that given on E, by setting $\alpha_i=X(\tilde{\alpha}_i)$ and $p_i=|D_{\tilde{\alpha}}X(\tilde{\alpha}_i)|\cdot\tilde{p}_i$, for $i\in J^h$.

Although the convergence theorem stated below holds for more general transformations X, the exposition is simplified, and the cases of practical interest are covered, by supposing that for each $b\in B$, the image of the circle $\{(b,\varphi):\varphi\in[0,2\pi]\}$ is a vortex filament in A. We denote again by η the vorticity field at time $t=0$, and define $c:A\to\mathbb{R}$ so that for each $\alpha\in A$,

$$c(\alpha)=|\eta(\alpha)|\,/\,|\partial_\varphi X(X^{-1}(\alpha))|\ .$$

where ∂_φ denotes differentiation in the φ direction. Thus, by hypothesis,

$$\eta(\alpha)=c(\alpha)\partial_\varphi X(X^{-1}(\alpha))\ .$$

Let ∂_φ^h be a discrete approximation to ∂_φ. These two operators can be pushed forward from E to A by defining, for functions $\Psi:A\to\mathbb{R}^3$,

$$\partial_\varphi\Psi(\alpha)=c(\alpha)\partial_\varphi(\Psi\circ X)(X^{-1}(\alpha))$$

and for $\Psi:\{\alpha_i\in A\}\to\mathbb{R}^3$,

$$\partial_\varphi^h\Psi(\alpha_i)=c(\alpha_i)\partial_\varphi^h(\Psi\circ X)(\tilde{\alpha}_i)$$

As a consequence of the above definition, we note that

$$\begin{aligned}\omega_\alpha(t)&=\left[D_\alpha\Phi(t)(\alpha)\right]\cdot\eta(\alpha)\\&=c(\alpha)\left[D_\alpha\Phi(t)(\alpha)\right]\cdot\partial_\varphi X(X^{-1}(\alpha))\\&=c(\alpha)\left[D_\alpha\Phi(t)(\alpha)\right]\cdot\left[D_\beta X(X^{-1}(\alpha))\right]\cdot\hat{\varphi}\\&=c(\alpha)\left[D_\beta(\Phi(t)\circ X)(X^{-1}(\alpha))\right]\cdot\hat{\varphi}\\&=c(\alpha)(\partial_\varphi(\Phi(t)\circ X)(X^{-1}(\alpha)))\\&=\partial_\vartheta\Phi(t)(\alpha)\,,\end{aligned}$$

where $\hat{\varphi}$ denotes the unit vector in the φ-direction.

The filament method whose convergence is stated in Theorem 5.1 consists of the system of ordinary differential equations

$$\Phi_i^{\delta,h}(0)=\alpha_i\,, \tag{5.12}$$

$$\frac{d}{dt}\Phi_i^{\delta,h}(t)=\sum_{j\in J^h}K_\delta(\Phi_i^{\delta,h}(t)-\Phi_j^{\delta,h}(t))\,\omega_i^{\delta,h}(t)\,p_j\,, \tag{5.13}$$

where

$$\omega_i^{\delta,h}(t)=\partial_\vartheta^h\Phi^{\delta,h}(t)(\alpha_i)\,. \tag{5.14}$$

Convergent filament methods which discretize sets of finitely many smooth, disjoint, vortex structures, each consisting of closed vortex filaments, can be obtained in this way.

Example: Consider a set of k vortex rings $A_1, \ldots, A_k$, with cross-sections identified with the pairwise disjoint sets $B_1, \ldots, B_k \subset \mathbb{R}^2$. The vortex rings may be unlinked or linked, knotted or not. Denote by X_i the natural identification $X_i: B_i\times[0,2\pi]\to A_i$. Set $A=\bigcup_{i=1}^{k}A_i$, $B=\bigcup_{i=1}^{k}B_i$, and $X=\bigcup_{i=1}^{k}:E=B\times[0,2\pi]\to A$. Observe that $|D_\beta X(\tilde{\beta})|=|\partial_\varphi X(\tilde{\alpha})|$ For simplicity in notation, we assume that $\partial_\varphi^h(\Psi)(\tilde{\alpha}_i)=\frac{\Psi_{i+1}-\Psi_{i-1}}{2h}$, although the proof of

Theorem 5.1 in fact requires that a difference method of higher order accuracy be employed. We have

$$\begin{aligned}\omega_i^{\delta,h}(t)p_i &= \partial_\varphi^h \Phi^{\delta,h}(t)(\alpha_i) \mid D_{\tilde{\alpha}} X(\tilde{\alpha}_i) \mid \tilde{p}_i \\ &= \frac{\mid \eta(\alpha_i) \mid}{\mid \partial_\varphi X(\tilde{\alpha}_i) \mid} \partial_\varphi^h (\Phi^{\delta,h}(t) \circ X)(\tilde{\alpha}_i) \mid D_{\tilde{\alpha}} X(\tilde{\alpha}_i) \mid h^3 \\ &= \partial_\varphi^h (\Phi^{\delta,h}(t) \circ X)(\tilde{\alpha}_i) \eta(\alpha_i) h^3 \\ &= \frac{\Phi_{i+h\varphi}^{\delta,h}(t) - \Phi_{i-h\varphi}^{\delta,h}(t)}{2h} \Gamma_i ,\end{aligned}$$

where $\Gamma_i = \eta(\alpha_i)h^3$. Thus, suppressing h and δ in the superscripts, equation (5.13) is transformed into the more familiar looking equation

$$\frac{d}{dt}\Phi_i(t) = \sum_j K_\delta(\Phi_i(t) - \Phi_j(t)) \left(\frac{\Phi_{j+h\varphi}(t) - \Phi_{j-h\varphi}(t)}{2h}\right) \Gamma_j$$

Theorem 5.1 Assume that ∂_φ^h is an r^{th}-order accurate centered difference operator. Let h, δ, and Δt be sufficiently small, with h sufficiently smaller than δ, and assume $l \geq 4$, $r \geq 4$. Then the solutions of the system (5.12)-(5.14) converge to the exact particle trajectories, and when integrated in time by a Runge-Kutta method of order $m=1$ or $m=2$, the error can be estimated by

$$\| e(t) \|_{L_h^2(A)} \leq C(\delta^p + h^l \delta^{1-l} + h^r + \Delta t^m) ,$$

where $e(t)(\alpha_i) = \Phi_{\alpha_i}(t) - \Phi_i^{\delta,h}(t)$.

Sketch of Proof: This theorem can be proved in the same way as convergence of the mesh algorithm is proved, once stability and consistency estimates have been obtained.

As a preliminary, we define the following Lagrangian functions on the variables $\tilde{\alpha}$. For $\Psi, \Omega : A \to \mathbb{R}^3$, set

$$V[\Psi,\Omega](\tilde{\alpha}) = U[\Psi \circ X, \Omega \circ X](\Psi(X(\tilde{\alpha}))) ,$$

and for $\Psi,\Omega:\{\alpha_i \in A\} \to \mathbb{R}^3$, define

$$V_{\delta,h}[\Psi,\Omega](\tilde{\alpha}_i) = U_{\delta,h}[\Psi \circ X, \Omega \circ X](\Psi(\alpha_i)) .$$

Consistency:

Observe that the integration formula on A is of the same order of accuracy as the integration formula on E from which it is inherited. For, if $F:A \to \mathbb{R}$ is a smooth function, then

$$\begin{aligned} \left| \int_A F(\alpha) d\alpha - \sum_{i \in J^h} F(\alpha_i) p_i \right| &= \left| \int_E F(X(\tilde{\alpha}))(|D_{\tilde{\alpha}} X|(\tilde{\alpha})) d\tilde{\alpha} \right. \\ &\quad \left. - \sum_{i \in J^h} F(X(\tilde{\alpha}_i))\,(|D_{\tilde{\alpha}} X|(\tilde{\alpha}_i))\,\tilde{p}_i \right| \\ &= \left| \int_E G(\tilde{\alpha}) d\tilde{\alpha} - \sum_{i \in J^h} G(\tilde{\alpha}_i) \tilde{p}_i \right| , \end{aligned}$$

where $G = (F \circ X) \cdot |D_{\tilde{\alpha}} X|$. By Theorem 1.1, we have

$$\| U[\Phi(t),\omega(t)] - U_{\delta,h}[\Phi(t),\omega(t)] \|_{L^\infty(\mathbb{R}^3)} \le C(\delta^p + h^l \delta^{1-l}) . \tag{5.15}$$

It follows from (5.15) and the boundedness of E that for some constant C,

$$\| V[\Phi(t),\omega(t)] - V_{\delta,h}[\Phi(t),\omega(t)] \|_{L^2_h(E)} \le C(\delta^p + h^l \delta^{1-l}) . \tag{5.16}$$

Stability:

The stability result (5.2) of Beale and Majda can be extended to the present case. Thus,

$$\begin{aligned} \| V_{\delta,h}[\Phi(t),\omega(t)] - V_{\delta,h}[\Psi,\Omega] \|_{L^2_h(E)} \le C(&\| \Phi(t) \circ X - \Psi \circ X \|_{L^2_h(E)} \\ &+ \| \omega(t) - \Omega \|_{W_h^{-1,2}(E)}) . \end{aligned} \tag{5.17}$$

for Ψ and Ω sufficiently close to $\Phi(t)$ and $\omega(t)$, respectively. We omit the details. In order to obtain an $L^2_h(E)$ norm estimate for $V_{\delta,h}[\Phi(t),\omega(t)] - V_{\delta,h}[\Phi^{\delta,h}(t),\omega^{\delta,h}(t)]$, we observe that

$$
\begin{aligned}
|\omega_i^{\delta,h}(t)-\omega_{\alpha_i}(t)| &= |\partial_\vartheta^h\Phi^{\delta,h}(t)(\alpha_i)-\partial_\vartheta\Phi^{\delta,h}(t)(\alpha_i)| \\
&= |c(\alpha_i)|\,|\partial_\varphi^h(\Phi^{\delta,h}(t)\circ X)(\tilde{\alpha}_i)-\partial_\varphi(\Phi(t)\circ X)(\tilde{\alpha}_i)| \\
&\le |c(\alpha_i)|\,(|\partial_\varphi^h(\Phi^{\delta,h}(t)\circ X)(\tilde{\alpha}_i)-\partial_\varphi^h(\Phi(t)\circ X)(\tilde{\alpha}_i)| \\
&\quad + |\partial_\varphi^h(\Phi(t)\circ X)(\tilde{\alpha}_i)-\partial_\varphi(\Phi(t)\circ X)(\tilde{\alpha}_i)|)\,.
\end{aligned}
$$

Since $\Phi(t)\circ X$ is a smooth function with *a priori* bounds on its derivatives for $0\le t\le T$,

$$
\|\partial_\varphi^h(\Phi(t)\circ X)-\partial_\varphi(\Phi(t)\circ X)\|_{W_h^{-1,2}(E)} \le Ch^r\,.
$$

Furthermore, it follows from the stability of the difference operator ∂_φ^h that

$$
\|\partial_\varphi^h((\Phi^{\delta,h}(t)\circ X)-(\Phi(t)\circ X))\|_{W_h^{-1,2}(E)} \le C\,\|(\Phi^{\delta,h}\circ X)-(\Phi(t)\circ X)\|_{L_h^2(E)}\,.
$$

Thus,

$$
\|\omega^{\delta,h}(t)-\omega(t)\|_{W_h^{-1,2}(E)} \le C(\|\Phi^{\delta,h}(t)-\Phi(t)\|_{L_h^2(E)}+h^r)\,,
$$

where C is independent of h and δ.

Hence,

(5.18)

$$
\|V_{\delta,h}[\Phi(t),\omega(t)]-V_{\delta,h}[\Phi^{\delta,h}(t),\omega^{\delta,h}(t)]\|_{L_h^2(E)} \le C(\|\Phi(t)-\Phi^{\delta,h}(t)\|_{L_h^2(E)}+h^r)\,.
$$

Equations (5.16) and (5.18) yield, just as in the convergence proof for the mesh algorithm, that for some constant C and all $t\in[0,T]$,

$$
\|e(t)\circ X\|_{L_h^2(E)} \le C(\delta^p+(\frac{h}{\delta})^l+h^r+\Delta t^m)\,.
$$

Finally,

$$
\|e(t)\|_{L_h^2(A)} \le \|(|D_{\tilde{x}}X|)\|_{L^\infty(E)}\,\|e(t)\circ X\|_{L_h^2(E)}\,,
$$

which completes the proof.

Remark: The theorem as stated above assumes that the integration formula

used in each "cross-section" is the trapezoidal rule. In fact, any sufficiently accurate planar integration formula, in combination with the trapezoidal rule applied in the filamental direction, yields a convergent vortex method.

6. Modifications of the Methods.

In this section, we discuss modifications of the differential and discrete algorithms which attempt to remedy the loss of resolution due to vortex stretching and to incorporate the effects of viscosity.

After a reasonably short length of time has passed in a nontrivial fluid flow, material pieces of the fluid will have undergone stretching in some directions and contractions in others. Stretching of the fluid in the direction of the vorticity causes a decrease in resolution of the vorticity when vortex structures are resolved by finite numbers of vortices. Thus, a procedure is needed in vortex methods to add new vortices in places where the original ones have become too widely separated.

In the algorithms in which vorticity is determined by finite differences of the flow map, the interpolation of new vortices is straightforward. In those versions of the method in which filaments are tracked, one merely needs to choose a parameter which governs the maximum permitted inter-particle separation along the filament. Then, when the separation of any two neighboring particles exceeds this parameter, a new particle can be interpolated, by any reasonable interpolating procedure, between the two separated particles. In the mesh algorithm, similarly, new particles can be interpolated between too widely separated pairs of particles which were neighbors in any coordinate direction on the original mesh. In both cases, the finite difference operator governing the evaluation of vorticity can easily be modified, though high order accuracy may be lost.

In the differential algorithm, even if one assumes no knowledge of relative changes in position of nearby vortices, computations can also be refined through the addition of new vortices, though in a less natural and less accurate way. Once a value of vorticity $\omega_i^{\delta,h}(t)$ has become sufficiently large,

which suggests that the vortex filament to which $\omega_i^{\delta,h}(t)$ is tangent has become stretched, one can replace the vortex $(\Phi_i^{\delta,h}(t),\omega_i^{\delta,h}(t))$ by the two vortices $(\Phi_i^{\delta,h}\pm r,\ \frac{1}{2}\omega_i^{\delta,h}(t))$, where r is some parameter.

In 1973 ([10]), Chorin suggested solving the Navier-Stokes equations in two dimensions by adding to the convective motion of the vortices a random jump of variance $2\nu\Delta t$ at each time step, where Δt is the size of the time step and ν is the viscosity. In order to extend this idea to the calculations of three-dimensional vortex motion, Chorin ([11]) has suggested a discrete-update vortex method which can incorporate the effect of viscosity in this way. In his method, independent vortex segments are tracked. Each segment is determined by the positions of the particles at each of its two endpoints, and the vorticity is taken to be centered at the midpoint of the segment, with direction parallel to the segment, and with strength proportional to the length of the segment. Thus, vorticity is evaluated in the discrete stretching way. At each time step, in addition to the convective motion of the two ends of each segment, the segment as a whole makes a random jump.

It is pointed out in [2] that the same modeling of diffusion can be combined with the differential algorithms. At every time step, each vortex is convected by the velocity field due to all of the other vortices, and in addition makes a random jump. This viscous differential method differs from Chorin's method in that one only needs one fluid particle to resolve each piece of vorticity in the differential algorithm. Nevertheless, the computational work is roughly the same in the two methods, since the evaluation of the stretching term in the differential method requires as much computation as does the evaluation of the velocity, whereas the evaluation of the stretching in the finite difference methods requires an insignificant amount of work.

The simulation of diffusion by expansion of vortex cores, with characteristic core radius growing in time according to the solution of the linear heat equation, has also been proposed. Even in two dimensions, the core spreading algorithm can converge to the Navier-Stokes equations only for very special initial conditions. In three dimensions, core spreading is beset by additional difficulties.

Random walking can converge because the vortices, once diffused by their random jumps, continue to be convected by the velocity field. In cores spreading, on the other hand, there is no mechanism for the diffused vorticity to be correctly convected.

Let η be a two-dimensional vorticity distribution at time $t=0$, and assume the viscosity $\nu=1$. The core spreading algorithm converges, under appropriate smoothness conditions, to the system of equations

$$\tilde{\Phi}(\alpha,0)=\alpha$$

$$\frac{\partial}{\partial t}\tilde{\Phi}(\alpha,t)=\tilde{u}(\tilde{\Phi}(\alpha,t),t)$$

where

$$\tilde{u}(t)=K*(G_t*\xi(t))$$

$$\xi(\tilde{\Phi}(\alpha,t),t)=\eta(\alpha)$$

$$K(x)=(-x_2,x_1)/\,|x|^2$$

$$G_t(x)=\frac{1}{4\pi t}e^{-x^2/4t}$$

Set $\tilde{\omega}=\nabla\times\tilde{u}$. It can be checked by the reader that whereas the vorticity field given by the solution of the Navier-Stokes equation satisfies the equations

$$\omega(\alpha,0)=\eta(\alpha)$$

$$\frac{\partial\omega}{\partial t}=\Delta\omega-u\cdot\nabla\omega\,,$$

$\tilde{\omega}$ satisfies

$$\tilde{\omega}(\alpha,0)=\eta(\alpha)$$

$$\frac{\partial\tilde{\omega}}{\partial t}=\Delta\tilde{\omega}-G_\epsilon * (u\cdot\nabla\xi)$$

Thus, though the diffusion in the core spreading method is correct, the vorticity is convected not by the local velocity field, as it is in the Navier-Stokes equations, but by an averaged velocity. More details will be given elsewhere.

7. Desingularized Euler Equations

It is useful for the interpretation of the numerical results, and a better understanding of vortex methods, to introduce at this point a system of equations less singular than Euler's equations, obtained by modifying the relationship that holds between incompressible vector fields and their curls. Given one-parameter families of kernels K_δ as before, we call the system of equations

$$\begin{aligned} \omega(x,0)&=\eta(x) \\ \partial_t\omega+(u\cdot\nabla)\omega&=(\omega\cdot\nabla)u \\ u&=K_\delta * \omega \end{aligned} \tag{7.1}$$

the E_δ equations. There is a two-dimensional version of these equations (which have the same form as (7.1) except that the right-hand-side of the second equation is zero) for which it is easy to construct an existence theory following McGrath's existence theorem for Euler's equations based on the vorticity formulation ([28]). Moreover, as $\delta\to 0$, solutions of the modified equations converge to solutions of Euler's equations. In three dimensions, it is harder to construct solutions using the vorticity formulation, and I don't know how to prove existence of solutions to the E_δ equations. We shall assume, as is presumably true, that for all $\delta>0$, unique solutions to the system (7.1) exist on the time interval $[0,T]$, and that they converge, as $\delta\to 0$, to solutions of Euler's equations.

Denote by Φ^δ the flow map $\Phi^\delta:\mathbb{R}^3\times[0,T]\to\mathbb{R}^3$, uniquely determined by the equations

$$\lim_{\delta,h,1/n\to 0} \Phi^{\delta,h,n}(t) = \Phi(t)$$

are given for the mesh algorithm (3.3)-(3.7) one can satisfy the hypotheses of the convergence theorem by choosing δ and n to be appropriate functions of h. Thus, in principle, one can implement a converging numerical procedure by evaluating $\Phi^{\delta(h),h,n(h)}(t)$ for h tending to 0. For example, Beale and Majda suggested setting $\delta(h)=h^q$ for some $q\in(0,1)$.

Unfortunately, the approximation of $\Phi(t)$ by $\Phi^{h^q,h}(t)$ is difficult numerically, because the ordinary differential equations are stiff when h is just slightly smaller than δ, and hence (as the experience of various workers indicates) unreasonably small values of h may be needed to obtain approximations $\Phi^{h^q,h}(t)$ close to $\Phi(t)$. The natural procedure to carry out in computing is

$$\lim_{\delta\to 0}\lim_{h\to 0}\lim_{n\to\infty} \Phi^{\delta,h,n}(t) = \Phi(t)\,.$$

That is to say, for fixed h and δ one decreases the size of the time steps until $\Phi^{\delta,h}$ is obtained with sufficient accuracy. Then one decreases h until Φ^{δ} is computed accurately enough. Finally one decreases δ to approach Φ. As a consequence of the increasing singularity of K_δ with decreasing δ, smaller h is needed for $\Phi^{\delta,h}$ to approximate Φ^{δ} accurately and larger n is required for $\Phi^{\delta,h,n}$ to approximate $\Phi^{\delta,h}$. With a given limit on how much computing one is able to do, one terminates the numerical experiments when a value of δ is reached which is so small that convergence in h cannot be obtained.

For sufficiently smooth flows and sufficiently small time intervals, one can compute $\Phi^{\delta}(t)$ accurately for δ small enough so that one can observe computationally pointwise convergence to $\Phi(t)$ ([20]). In general, this cannot be done for more complicated flows. However, this does not mean that insight cannot be gained from computations of Φ^{δ} in these flows. An example is provided by Anderson's calculations ([1]) of an interface between fluids of slightly different densities, with vorticity smoothed by two-dimensional core

functions depending on a parameter δ. Although he was unable to observe pointwise convergence in δ everywhere, very interesting behavior was observed for a sequence of values of δ, with convergence occurring pointwise over a larger and larger part of the fluid. Moreover, the nature of the numerical solutions for the range of values of δ over which Anderson computed suggests fascinating, intricate behavior of the limiting (δ=0) solution.

8. Ring Merger.

We consider now the the short time evolution of vorticity which is initially concentrated in two identical, axisymmetric vortex rings of the same sign and lying in a common plane. The initial distribution of vorticity is determined by the radius ρ_R of the rings, the separation ρ_S of the ring centers, and the core shape $\xi:[0,\rho_C]\to\mathbb{R}$ which describes the initial vorticity strength in each ring cross-section as a function of distance from the center of the core (ρ_C denotes the core radius, and we assume that $\rho_C \ll \rho_R$). Thus, each ring is a translate of the vortex ring centered at the origin, with central core lying in the (x,y)-plane, and defined by the initial vorticity function

$$\eta_0(x)=\xi(\sqrt{(r-\rho_R)^2+x_3^2}\,)\,(\sin(\vartheta),-\cos(\vartheta),0)\,,$$

where

$$r=\sqrt{x^2+y^2} \qquad\qquad \vartheta=\arctan(\frac{y}{x})$$

We assume that the coordinate axes are so chosen that the ring centers are equidistant from the origin on the y-axis, at the positions $c_+=(0,\frac{1}{2}\rho_s,0)$ and $c_-=-c_+$. Thus, the initial distribution of vorticity is the vector field η, where

$$\begin{aligned}\eta(x)&=\eta_+(x)+\eta_-(x)\\ &=\eta_0(x-c_+)+\eta_0(x-c_-)\end{aligned}$$

We call the corresponding rings R_+ and R_-.

Let x be a point in one of the two rings, say R_+. The velocity field at x at time $t=0$ is

$$(K*\eta)(x)=(K*\eta_+)(x)+(K*\eta_-)(x)\,.$$

The term $(K*\eta_+)(x)$, for $x\in R_+$, is close to being a sum of a uniformly downward velocity and a rotation about the core. Thus, over a reasonably short

interval of time, and in the absence of the neighboring ring, the vorticity in R_+ is translated downward, for the rotational component of the flow does not change the distribution of vorticity. The other term $K * \eta_-$ imparts an upward component of velocity to R_+. This velocity is of course not uniform over the entire ring; the effect is most pronounced on the edge of R_+ closest to R_-. Hence, after the initial instant of time, the rings become distorted and are no longer planar. The upward tilt of the nearby edges of the rings creates a component of velocity in the direction joining the two rings, and they move close together. The velocity field due to the vorticity in the near edges of the two rings, which are almost tangent to one another (see the first column in figures 9.1-9.3) and of opposite circulation, is negligible except very near these edges, for the two opposite lines of vorticity contribute velocities which cancel each other. Each edge, however, imparts an upward component of velocity to the other. The remaining vorticity forms essentially one vortex ring (though a nonplanar one), which we call the merged ring. From a side view (see, for example, the second column of figures 9.1-9.3) this ring forms almost an upside-down V-shape, with the two halves of the V coming from the two original rings. This V-shaped structure has a fairly strong self induced motion away from the center of the two-ring structure (that is, in the x-direction). Thus, the adjacent ring sections become stretched by large factors and hence come even closer together. One result of this stretching is that a substantial amount of the vorticity is now occupied by a very small portion of the original vortex rings. When viscosity is considerable, the nearby edges will diffuse into one another and the vorticity in this part of the fluid will be very much diminished.

Calculations of the inviscid interaction of two rings are described in the next two sections. We have taken the rings to be not coplanar, but rather

inclined toward one another by 15° (as in the Schatzle experiments ([33]). There is a good reason for this nonplanar choice of initial condition in computational experiments, for the interaction between the two rings occurs much more quickly when they are already moving toward one another at time $t=0$, and a higher proportion of the computational labor can be used to resolve the interaction process. There is some sensitivity to the choice of initial angle of inclination, but the qualitative development is the same.

In the computations reported in Sections 9 and 10, the centers of the two rings were separated by 0.23, the initial radius of each ring was .088, and the weights of the vortices were scaled so that the total vorticity (L^1 norm) of each ring was 20.

The filament method of the type described in Section 3 was used, with a second-order centered difference to evaluate the vorticity, and a third-degree polynomial interpolation procedure to introduce new particles between pairs of particles which have become too widely separated. The cutoff function used is the characteristic function of the unit ball, scaled appropriately. The ordinary differential equations were integrated in time by a second-order Runge-Kutta method.

9. Computations with Single Filaments.

Interesting features of the ring merger process can be gleaned from calculations which require very little computing time. The set of numerical experiments described in this section involves representation of the vorticity in each of the two rings by a single discretized filament. The cutoff functions used are three-dimensional and radially symmetric. Since singular lines of vorticity have infinite self-induced velocities, one cannot look at the δ=0 limit. Rather, we investigate the behavior of the rings over a range of moderate values of δ. Whereas singular filaments have infinite velocities in Euler's equations, the velocities in E_δ of singular filaments are finite.

With fixed δ, as the resolution along the two filaments is increased, the computed solution converges to a weak solution of the E_δ system. The filament configurations displayed in figures 9.1-9.3 are accurate approximate weak solutions of the E_δ system; refinements in the size of the time steps and in the number of particles followed in each filament cause negligible changes in the solution.

The pictures displayed are perspective views, from four different perspectives, of the vortex rings. The arrows pictured in the last two columns are the velocity vectors emanating from the vortex positions, and in each of these last two columns, one of the rings has been suppressed. Both the arrows and the filaments are drawn by projection of these objects onto a plane between a viewer and the objects. With coordinate axes defined so that the rings lie initially in the (x,y)-plane, with centers on the y-axis, the viewers of the five columns are initially at the positions (1st column: $\hat{z}$, 2nd column: $\hat{x}$, 3rd and 4th columns: $\hat{x}+\hat{y}+\hat{z}$, 5th column: $\hat{y}$), and move with the center of mass of the ring system. Here $\hat{x}$ denotes the unit vector in the x-

direction, etc.

It is unenlightening in the singular filament calculation to compare computed solutions corresponding to different values of δ at the same instant of time. For, since the speeds of the rings increase greatly with decreasing δ, similar events occur much sooner with smaller values of δ. Thus, we can only compare the qualitative developments of the ring structures.

Even the qualitative development depends sensitively on the value of δ. The outer part of the rings induces a downward component of velocity on the adjacent edge pair which varies little with δ. However, the self-induced upward motion of the parallel pair of oppositely circulating vortex lines increases sharply as δ decreases. This effect is clearly discernible in figures 9.1-9.3.

In all of the runs, however, it can be seen that ring merger takes place in the following sense: the adjacent edges come so close together that their effect on distant portions of the ring structure is negligible. The remaining vorticity forms, with two small breaks, a (non-planar) ring of vorticity.

The mechanism by which ring merger occurs in viscous flow can perhaps already be deduced from these calculations. We see that the tremendous strain imposed on the adjacent edges, which is also observed in physical experiments ([33]), does not need viscosity or any specific vorticity distribution in the ring cores in order to take place. This strain could bring the edges sufficiently close together that viscosity can eliminate a large part of the vorticity there.

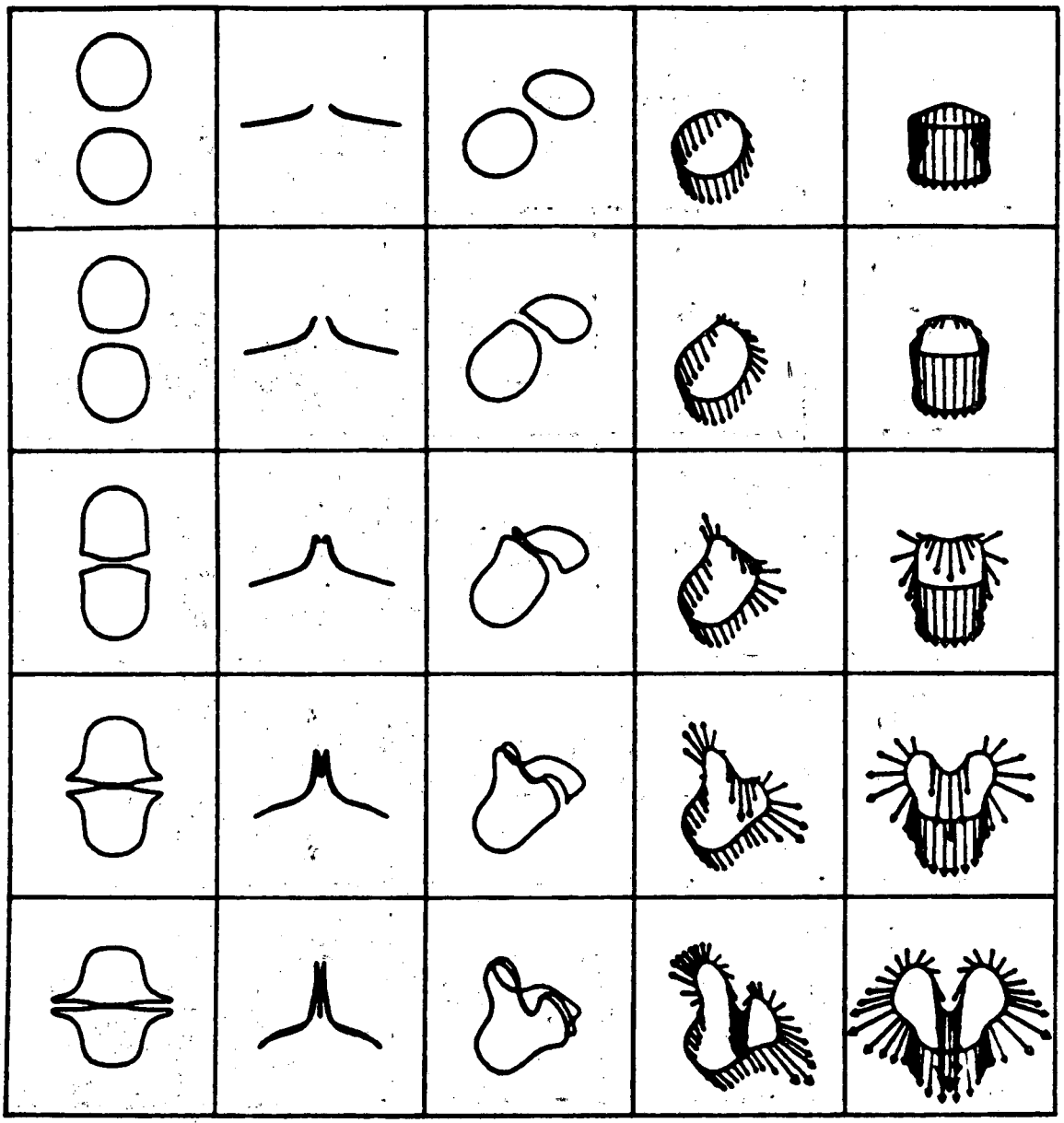

Figure 9.1

$\delta = .045$ $\Delta t = .00025$

steps: 4,8,12,16,20

times: 0.001, 0.002, 0.003, 0.004, 0.005

number of vortices: 24, 30, 33, 39, 54

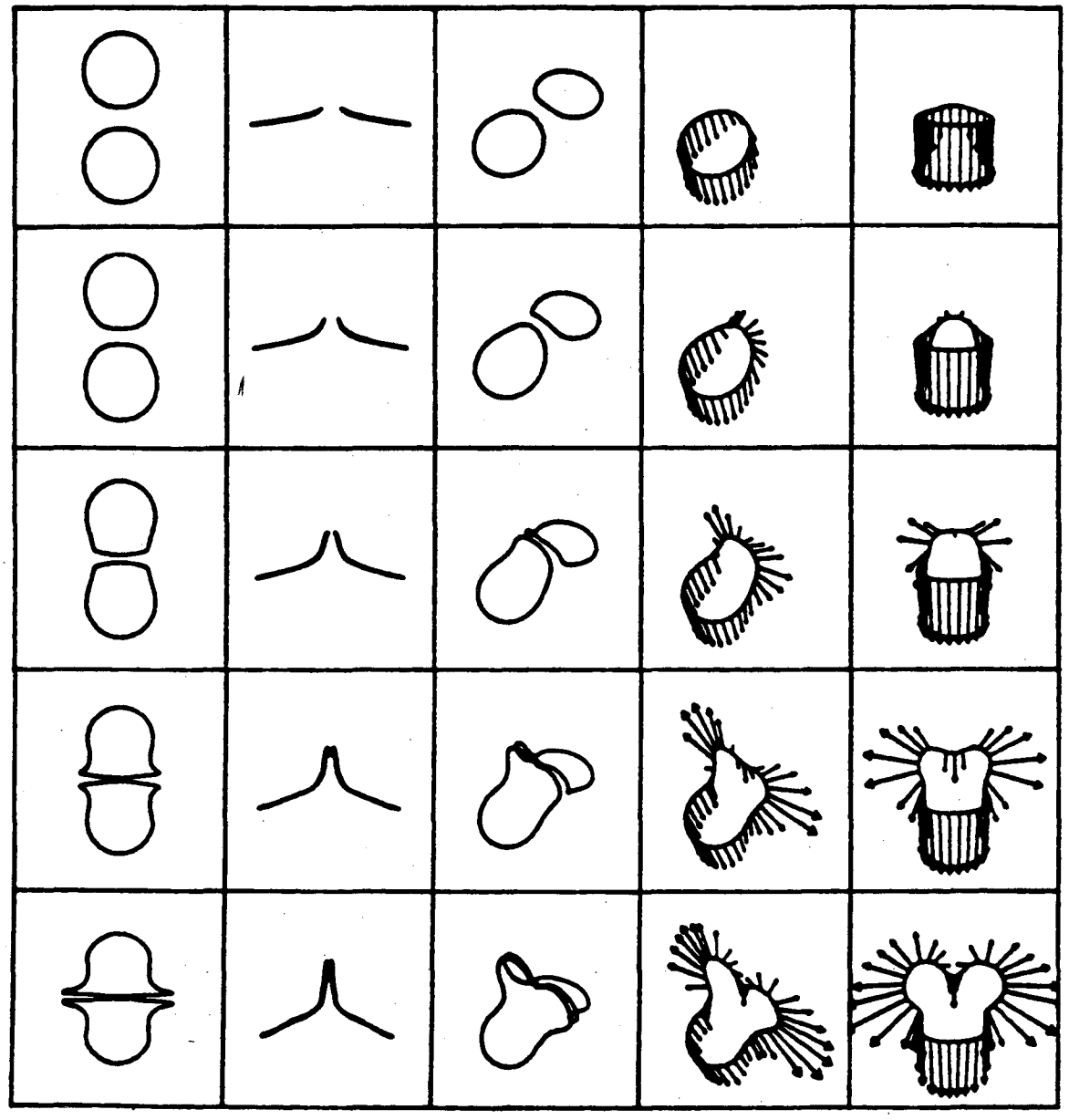

Figure 9.2

$\delta = .035$ $\Delta t = .00015$

steps: 5,10,15,20,25

times: 0.00075, 0.0015, 0.00225, 0.003, 0.00375

number of vortices: 24,28,31,37,44

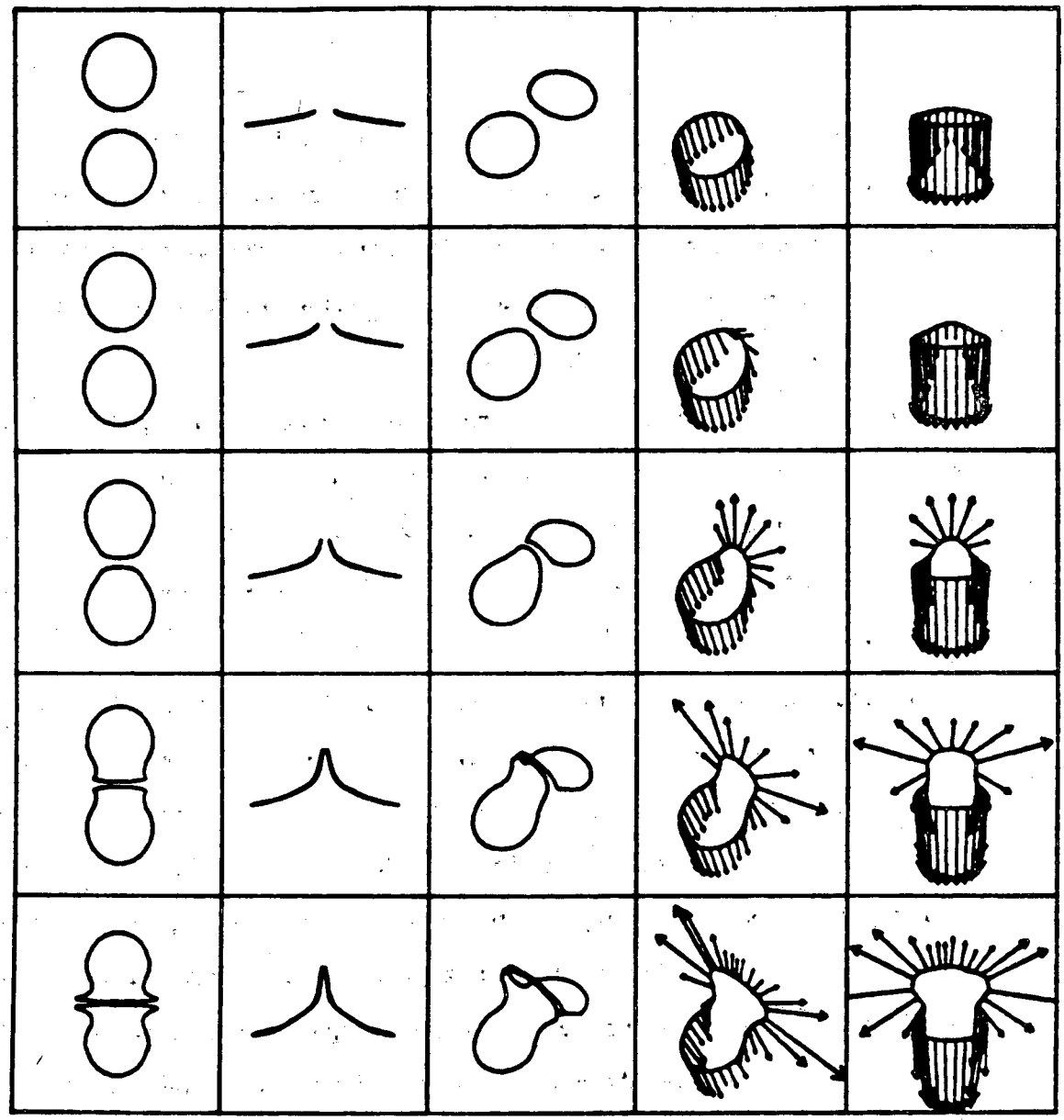

Figure 9.3

$\delta = .025$ $\Delta t = .0001$

steps: 5,10,15,20,25

times: 0.0005, 0.001, 0.0015, 0.002, 0.0025

number of vortics: 24,24,31,31,38

10. Computations with Full Cores.

The computations discussed in the previous section yielded convergent weak solutions of the E_δ equations. In this section, smooth solutions of the E_δ equations are provided. Unlike the singular filament case, solutions of the E_δ equations with cores of finite width do converge to solutions of Euler's equations on sufficiently short intervals of time.

The computations discussed here were carried out using the same filament method as in the last section, except that several filaments were used to resolve the cross-sections of the vortex rings. The ring radius and separation were as in Section 9; the core radius was .022 and the core function $\xi:[0,.022]\to\mathbb{R}$ (defined in Section 8) was given by $\xi(x)=\sqrt{(.022-x)/.022}$.

Figures 10.1-10.4 are perspective views from the positions (1st column: $\hat{z}$, 2nd column: $\hat{x}$, 3rd and 4th columns: $\hat{x}+\hat{y}+\hat{z}$) and the viewer, as in the previous section, is moving with the center of mass of the ring system. Only the central filament of each ring is drawn in the 3rd column, and the central filament of only one of the rings, with velocity field on that ring, is depicted in the 4th column. The figures are depictions of accurate solutions of the E_δ equations; refinements in the size of the time steps and increases in spatial resolution yield negligible changes, not only in the overall shape of the rings, but also in the position of the central filament and even in the velocity field at the central filament of the ring core.

Convergence of these solutions of the E_δ equations to solutions of Euler's equations is harder to see. We do obtain reasonable convergence in the center of mass, and the positions of the central filament of each ring also appear to converge. The central filaments in the $\delta=.02$ and $\delta=.015$ runs

differ very little. The point in a ring cross-section at which the cross-sectional component of velocity is zero is not at the center of the cross-section. The display of the velocity vectors in the final column of figure 10.4 shows a slight rotation of the central filament. This motion becomes observable only for small δ.

A rapidly increasing amount of computation is required to obtain accurate solutions of the E_δ equations as δ decreases. In fact, the computation depicted in figure 10.1 required less than five minutes on the VAX 11/780, while that in figure 10.4 took several minutes on the Cray 1. Of course, these computations can be continued to smaller values of δ, without drastic increases in expense, through improvements in efficiency of the algorithms (eliminating the square of the number of vortices operation count).

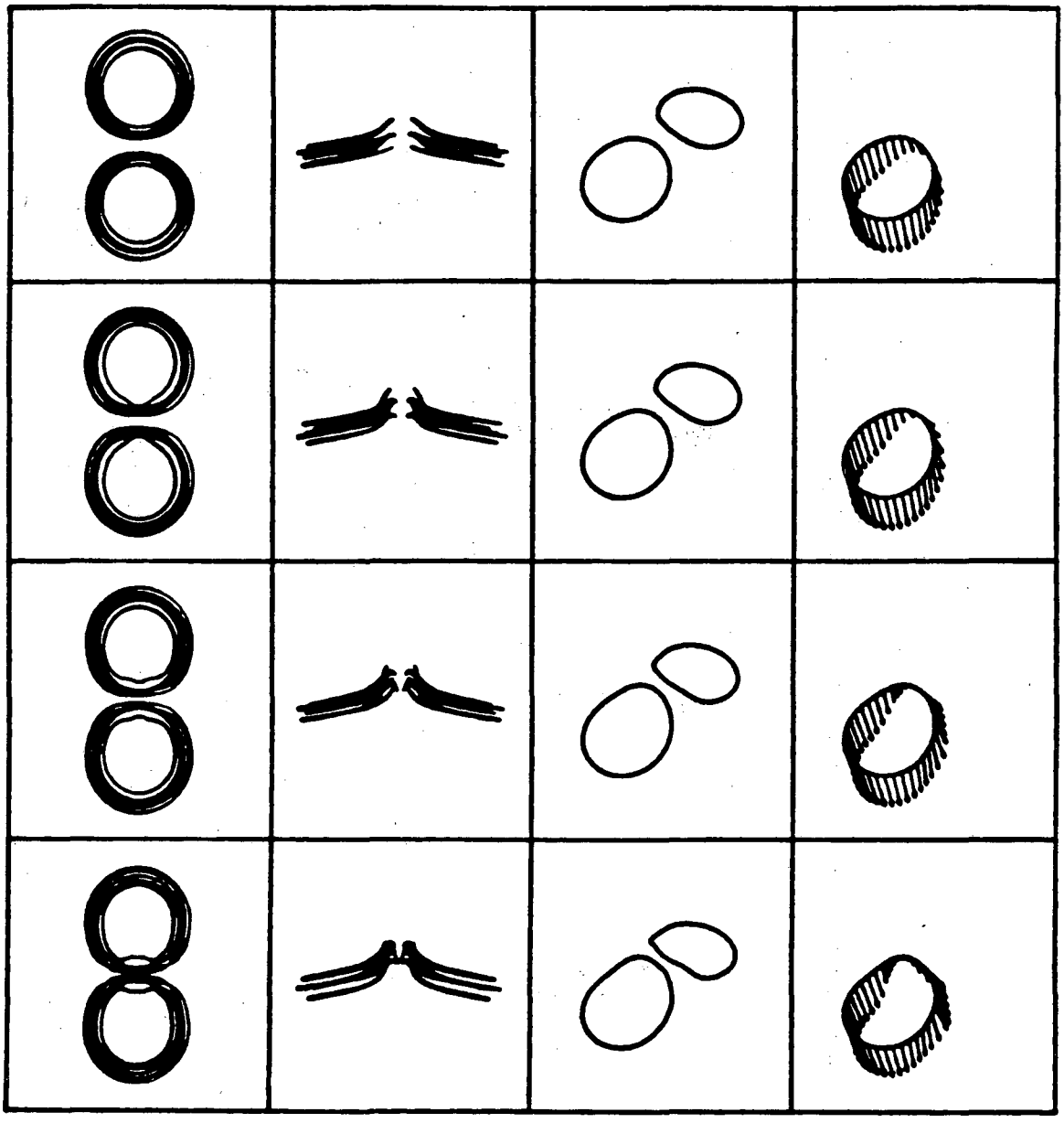

Figure 10.1

δ=.045 Δt=.0002

5 filaments per ring

steps: 5,7,9,11

times: 0.001, 0.0014, 0.0018, 0.0022

number of vortices: 225, 248, 258, 291

centers of mass: -.0311, -.0462, -.0592, -.0737

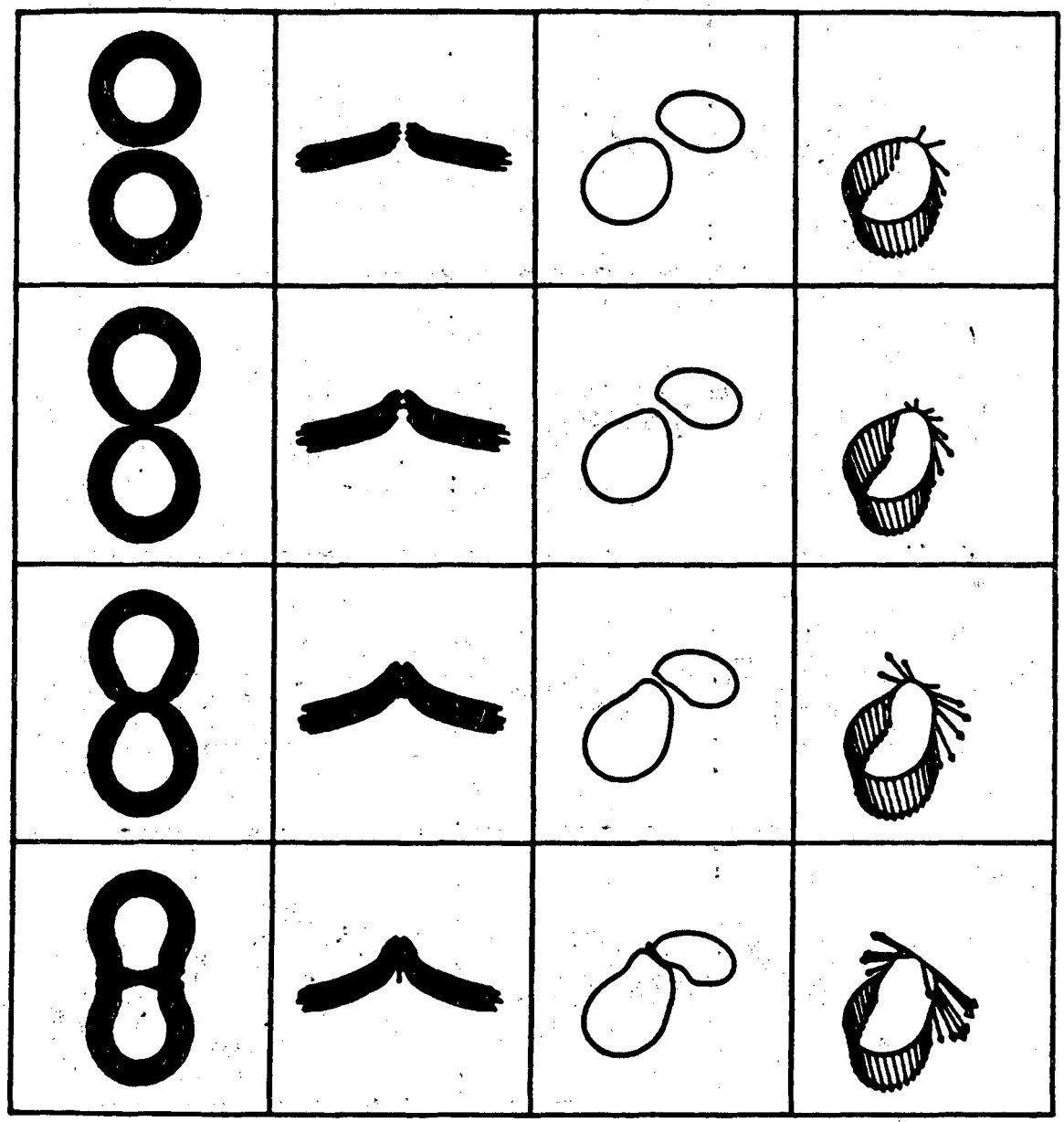

Figure 10.2

δ=.025 Δt=.0001

21 filaments per ring

steps: 10,14,18,22

times: 0.001, 0.0014, 0.0018, 0.0022

number of vortices: 684, 708, 738, 819

centers of mass: -.0420, -.0568, -.0693, -.0787

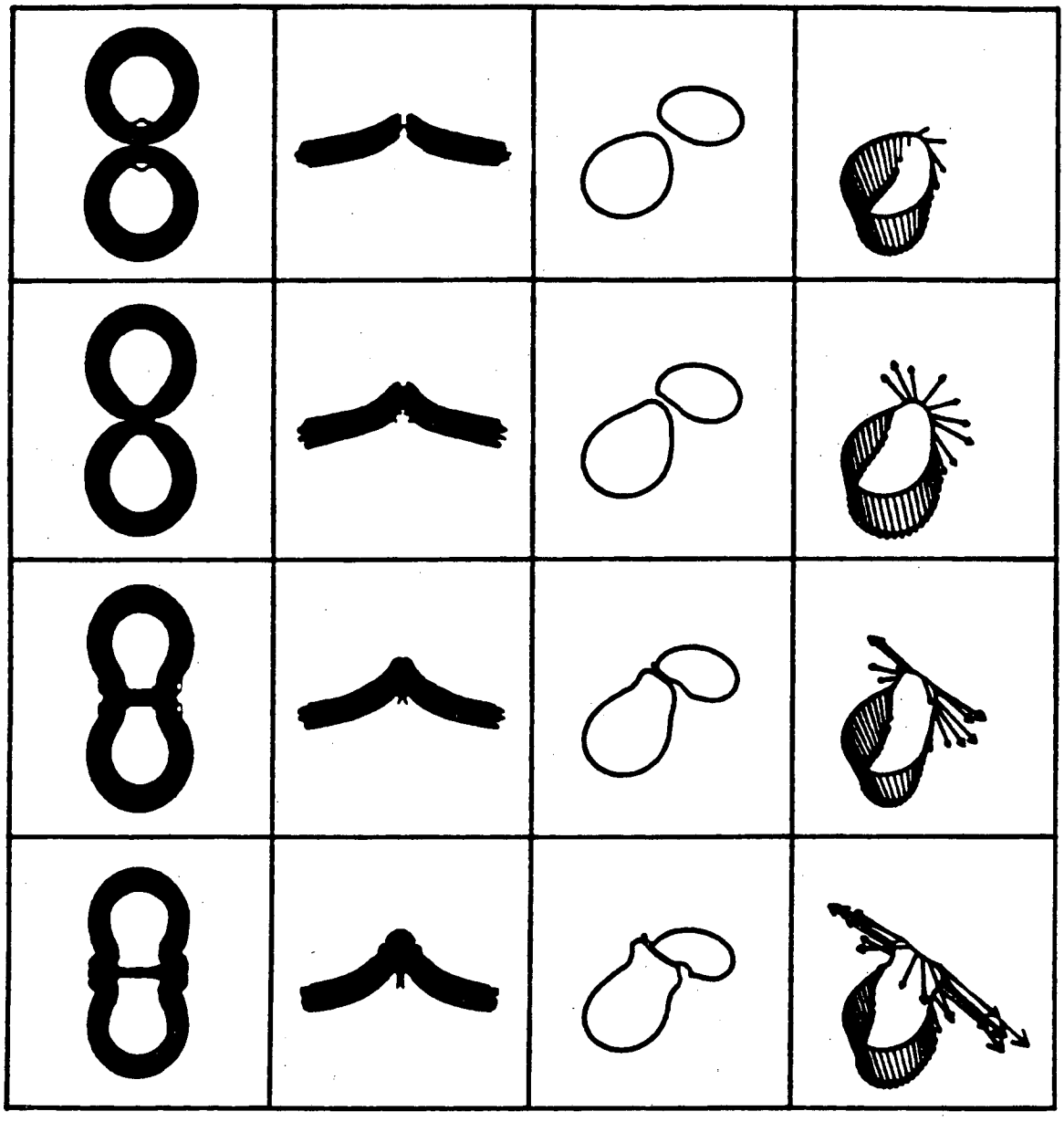

Figure 10.3

δ=.02 Δt=.00005

29 filaments per ring

steps: 20,28,36,44

times: 0.001, 0.0014, 0.0018, 0.0022

number of vortices: 1121, 1183, 1288, 153

centers of mass: -.0455, -.0596, -.0702, -.07

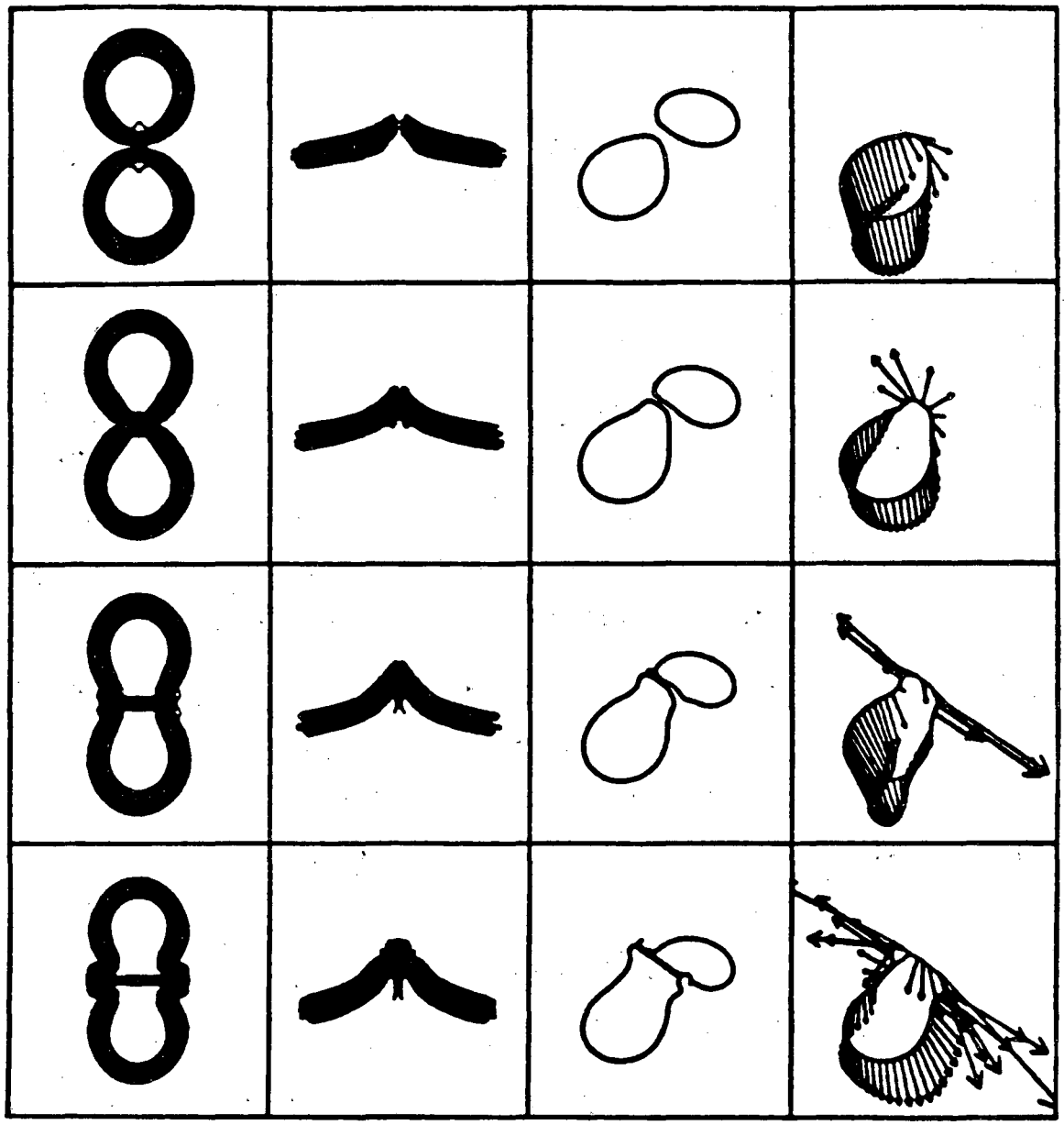

Figure 10.4

δ=.015 Δt=.00005

29 filaments per ring

steps: 20,28,36,44

times: 0.001, 0.0014, 0.0018, 0.0022

number of vortices: 1129, 1194, 1353, 1689

centers of mass: -.0475, -.0611, -.0712, -.0777

Bibliography

[1] C. Anderson , A vortex Method for Flows of Variable Density, submitted to J. Comp. Phys.

[2] C. Anderson and C. Greengard, On Vortex Methods, to appear in Siam J. Num. Analysis.

[3] W.T. Ashurst, Large Eddy Simulation via Vortex Dynamics, presented at the AIAA Sixth Computation Fluid Dynamics Conference, Danvers, MA 1983. AIAA Paper No. 83-1879-CP

[4] J.T. Beale and A. Majda, Rates of Convergence for Viscous Splitting of the Navier-Stokes Equations, Math. Comp., 37 (1981), pp.243-259.

[5] J.T. Beale and A. Majda, Vortex Methods I : Convergence In Three Dimensions, Math. Comp., 39 (1982), pp. 1-27.

[6] J.T. Beale and A. Majda, Vortex Methods II : Higher Order Accuracy in Two and Three Dimensions, Math. Comp., 39 (1982), pp. 29-52.

[7] J.T. Beale and A. Majda, Explicit Smooth Velocity Kernels and Vortex Method Accuracy, to appear in J. Comp. Phys..

[8] J.T. Beale, (private communication).

[9] A. Cheer, Numerical Study of Incompressible Slightly Viscous Flow Past Blunt Bodies and Airfoils, SIAM J. Sci. Stat. Comp., 4 (1983), pp. 685-705

[10] A.J. Chorin, Numerical Study of Slightly Viscous Flow, J. Fluid Mech., 57 (1973), pp. 785-796.

[11] A.J. Chorin, Vortex Models and Boundary Layer Instability, SIAM J. Sci. Stat. Comp., 1 (1980), pp. 1-21.

[12] A.J. Chorin, The Evolution of a Turbulent Vortex, Comm. Math. Phys., 83 (1982), pp. 517-533.

[13] A.J. Chorin and P.S. Bernard, Discretization of a Vortex Sheet, with an Example of Roll-up, J. Comp. Phys., 13 (1973), pp.423-429.

[14] A.J. Chorin and J. Marsden, A Mathematical Introduction to Fluid Mechanics, Springer-Verlag, New York, 1979.

[15] A.J. Chorin, T.J.R. Hughes, M.F. McCracken, and J.E. Marsden, Product Formulas and Numerical Algorithms, Comm. Pure Appl. Math., 31 (1978), pp. 205-256

[16] G.H. Cottet, These de 3eme cycle (to appear).

[17] G.H. Cottet, and P.A. Raviart, Particle Methods for One- Dimensional Vlasov-Poisson Equations, SIAM J. Num. Anal., 21 (1984),pp. 52-76.

[18] B. Couet, O. Buneman, and A. Leonard, Simulation of Three-Dimensional Incompressible Flows with Vortex-in-Cell Method, J. Comp. Phys., 39 (1981), pp.305-328

[19] A.F. Ghoniem, A.J. Chorin, and A.K. Oppenheim, Numerical Modelling of Turbulent Flow in a Combustion Tunnel, Phil. Trans. R. Soc. Lond. A, 304 (1982), pp. 303-325

[20] O.H.Hald and V. Mauceri Del Prete, Convergence of Vortex Methods for Euler's Equations, Math. Comp., 32 (1978), pp.791,809

[21] O. Hald, The Convergence of Vortex Methods, II., SIAM J. Num. Anal., 16 (1979), pp. 726-755.

[22] T. Kato, Nonstationary Flows of Viscous and Ideal Fluids in R^3, J. Funct. Anal., 9 (1972), pp.296-305.

[23] R. Krasny, A Numerical Study of Kelvin-Helmholtz Instability by the Point Vortex Method, Ph.D. Thesis, Department of Mathematics, University of California at Berkeley, (1983).

[24] A. Leonard, Numerical Simulation of Interacting Three Dimensional Vortex Filaments, Proc. 4th Int. Conf. on Num. Methods in Fluid Dynamics., R.D. Richtmeyer, ed., Springer-Verlag, New York, 1975, pp.245-250.

[25] A. Leonard, Vortex Methods for Flow Simulation, Journal of Computational Physics, 37 (1980), pp. 289-335

[26] A. Leonard, Computing Three-Dimensional Incompressible Flows with Vortex Elements, to appear in Annual Review of Fluid Mechanics, vol. 17, 1985

[27] C. Marchioro and M. Pulvirenti, Hydrodynamics in Two Dimensions and Vortex Theory, Comm. Math. Phys., 84 (1982), pp. 483-503

[28] F.J. McGrath, Nonstationary Plane Flow of Viscous and Ideal Fluids, Arch. Rational Mech. Anal., (1968), pp. 329-348.

[29] M. McCracken and C. Peskin, Vortex Methods for Blood Flow Through Heart Valves, J. Comp. Phys., 35 (1980), pp.183-205

[30] Y. Nakamura, A. Leonard, and P.R. Spalart, Numerical Simulation of Vortex Breakdown by the Vortex-Filament Method, AGARD Proceedings #342, Rotterdam, April 1983.

[31] Y. Oshima and S. Asaka, Interaction of two Vortex Rings Along Parallel Axes in Air, Jour. Phys. Soc. Japan, 42 (1977), pp. 708-713.

[32] M. Perlman, On the Accuracy of Vortex Methods, to appear in Jour. Comp. Phys. (1984).

[33] P. Schatzle, (private communication).

[34] J. Sethian, Turbulent Combustion in Open and Closed Vessels, J. Comp. Phys., 54 (1984), pp. 425,456

[35] S. Shirayama and K. Kuwahara, Proceedings Ninth International Conference on Numerical Methods in Fluid Dynamics, June 1984, Saclay,

France, to be published by Springer-Verlag in Lecture Notes in Physics.

[36] P.R. Spalart, Numerical Simulation of Separated Flows, Ph.D. Thesis, Department of Aeronautics and Astronautics, Stanford University, (1982).

This report was done with support from the Department of Energy. Any conclusions or opinions expressed in this report represent solely those of the author(s) and not necessarily those of The Regents of the University of California, the Lawrence Berkeley Laboratory or the Department of Energy.

Reference to a company or product name does not imply approval or recommendation of the product by the University of California or the U.S. Department of Energy to the exclusion of others that may be suitable.

TECHNICAL INFORMATION DEPARTMENT
LAWRENCE BERKELEY LABORATORY
UNIVERSITY OF CALIFORNIA
BERKELEY, CALIFORNIA 94720